

April 2013

# Developing a Biosensor to Monitor Glioblastoma

Ana M. Dede Dukaj  
*Worcester Polytechnic Institute*

Courtney Anne Rosales  
*Worcester Polytechnic Institute*

Nesa-Maria Ashley Anglin  
*Worcester Polytechnic Institute*

Thomas Gregory Jones  
*Worcester Polytechnic Institute*

Follow this and additional works at: <https://digitalcommons.wpi.edu/mqp-all>

---

## Repository Citation

Dede Dukaj, A. M., Rosales, C. A., Anglin, N. A., & Jones, T. G. (2013). *Developing a Biosensor to Monitor Glioblastoma*. Retrieved from <https://digitalcommons.wpi.edu/mqp-all/926>

This Unrestricted is brought to you for free and open access by the Major Qualifying Projects at Digital WPI. It has been accepted for inclusion in Major Qualifying Projects (All Years) by an authorized administrator of Digital WPI. For more information, please contact [digitalwpi@wpi.edu](mailto:digitalwpi@wpi.edu).

# Development of a Biosensor to Monitor Glioblastoma

---

Nésa-Maria Anglin  
Ana Dede  
Thomas Jones  
Courtney Rosales

Anjana Jain, Ph.D.  
Department of Biomedical Engineering

Suzan Zhou, Ph.D.  
Department of Chemical Engineering

**Major Qualifying Project  
2012-2013  
Department of Biomedical Engineering  
Worcester Polytechnic Institute**

# Table of Contents

Authorship .....	9
Acknowledgements.....	10
Abstract.....	11
Chapter 1            Introduction .....	12
1.1    Background .....	13
1.2    Design.....	13
1.3    Methodology for Prototype Development and Validation.....	14
1.4    Results.....	16
1.5    Discussion.....	16
Chapter 2            Background and Literature Review .....	18
2.1    Introduction .....	19
2.2    Biology of Cancer .....	22
2.2.1 Cell Metabolism .....	22
2.2.2 Role of Altered Cell Metabolism in Cancer .....	23
2.2.3 Cell Metabolism of Glioblastoma Multiforme .....	26
2.3    Biosensors .....	28
2.3.1 History of Biosensors .....	28
2.3.2 Current Applications .....	30
2.3.3 Design Criteria.....	30
2.3.3.1 Selectivity .....	31
2.3.3.2 Sensitivity .....	32
2.3.3.3 Stability .....	34
2.3.3.4 Biofouling .....	35
2.3.3.5 Response Time .....	35
2.3.3.6 Sensing Capability Tradeoff .....	36
2.3.4 Biosensor Coatings.....	36
2.3.4.1 Conductive Films .....	38
2.3.4.1.1 Polyaniline (PANI) .....	39
2.3.4.1.2 Polypyrrole (PPy).....	40
2.3.4.2 Non-conductive Coatings.....	41

2.3.4.3 Multilayer Nanofilms .....	42
2.3.4.4 Enzyme-immobilization Technologies .....	44
Chapter 3            Design Process .....	47
3.1    Project Basics .....	48
3.1.1            Project Stakeholders .....	48
3.1.2            Initial Statement.....	48
3.1.3            Revised Client Statement .....	48
3.2    Objectives.....	49
3.2.1            Primary Objectives .....	50
3.2.2            Secondary Objectives.....	50
3.3    Constraints .....	51
3.4    Project Approach .....	52
3.4.1    Research.....	52
3.4.2    Design.....	52
a.    Identifying Design Criteria.....	53
b.    Generating Design Alternatives and Selecting a Design .....	53
3.4.3    Prototyping .....	53
3.4.4    Testing.....	54
3.4.5    Design Reiteration and Documentation .....	55
Chapter 4            Design Process .....	56
4.1    Need Analysis.....	57
4.2    Functions.....	58
4.3    Specifications .....	60
4.3.1    Metabolites .....	60
4.3.2    Biorecognition and transduction agent .....	60
4.3.3    Sensitivity and Range .....	61
4.3.4    Dimensions.....	61
4.3.5    Stability .....	61
4.4    Design Alternatives .....	61
4.4.1    Developing Design Alternatives .....	62
4.4.2    Design Alternatives .....	62
1: Mushroom.....	63

2: CNT Towers .....	64
3: CNT Bed.....	65
4: Smart Polymer .....	65
5: Single Layer .....	66
6: Bilayer.....	66
7: Tri-layer.....	67
8: Single Layer with Surface Indentations.....	67
9: Nanovelcro.....	68
10: One Enzyme Mushroom .....	68
11: One Enzyme Single Layer .....	69
12: One Enzyme Bilayer .....	69
4.5 Design Alternative Evaluation.....	70
4.5.1 Evaluation of Materials .....	70
4.5.2 Evaluation of Design Alternatives .....	70
4.5.2.1 Monitoring Ability .....	71
4.5.2.2 Manufacturability .....	71
4.5.2.3 Interference Reduction .....	72
4.5.2.4 Cost .....	72
4.5.3 Final Design Alternative Scores.....	72
4.6 Final Design .....	73
Chapter 5 Methodology .....	80
5.1 Film deposition.....	81
5.2 Film characterization.....	82
5.2.1 Contact angle analysis.....	82
5.2.2 Cyclic voltammetry.....	83
5.3 Bench biosensor validation .....	83
5.3.1 Lactate amperometry .....	83
5.3.2 Real time lactate recognition.....	84
5.4 <i>In vitro</i> biosensor validation.....	84
5.4.1 Cell Culture.....	85
5.4.2 Colorimetric assay.....	85
5.4.3 Biosensor experiments .....	85

Chapter 6	Results.....	86
6.1	Film Characterization .....	87
6.1.1	Contact Angle Analysis.....	87
6.1.2	Cyclic Voltammetry .....	87
6.2	Bench biosensor validation.....	88
6.2.1	Lactate Amperometry .....	88
6.2.2	Real-time Lactate Recognition .....	89
6.3	<i>In Vitro</i> Biosensor Validation .....	90
6.3.1	Colorimetric Assay .....	90
6.3.2	In Media .....	91
Chapter 7	Discussion .....	92
7.1	Design Validation .....	93
7.2	Project Considerations .....	94
7.2.1	Economy.....	94
7.2.2	Environment.....	95
7.2.3	Social influence .....	95
7.2.4	Ethics .....	95
7.2.5	Health and Safety .....	95
7.2.6	Manufacturability .....	96
Chapter 8	Conclusion and Future Recommendations.....	97
8.1	Conclusions .....	98
8.2	Measure Glutamate Levels .....	99
8.3	Incorporate Horseradish Peroxidase .....	99
8.4	Add Outer Chitosan Layer.....	100
8.5	Miniaturize Electrode System .....	100
References	.....	101
Appendices.....		110
Appendix 3.A:	Objectives tree for Cancer Metabolite Biosensor.....	111
Appendix 3.B:	Pairwise comparison chart of the primary objectives. ....	112
Appendix 3.C:	Pairwise comparison chart of the secondary objectives. ....	113
Appendix 4.A:	Functions-Means Chart .....	114
Appendix 4.B:	Material Evaluation .....	115

Appendix 4.C:	Monitoring Ability Evaluation .....	117
Appendix 4.D:	Manufacturability Evaluation.....	119
Appendix 4.E:	Interference Evaluation .....	120
Appendix 4.F:	Cost Evaluation .....	121
Appendix 5.A:	Protocol for Polypyrrole Deposition .....	123
Appendix 5.B:	Contact Angle Analysis .....	125
Appendix 5.C:	Cyclic Voltammetry .....	126
Appendix 5.D:	Lactate Amperometry .....	127
Appendix 5.E:	Real Time Lactate Recognition.....	128
Appendix 5.F:	Colorimetric Lactate Assay.....	129
Appendix 5.G:	Biosensor in Media.....	130

# Table of Figures

Figure 1: Illustration highlighting the differences between oxidative phosphorylation, anaerobic glycolysis, and the Warburg effect through aerobic glycolysis [15].	24
Figure 2: Above is a hierarchical illustration of the metabolic pathways and specific metabolites affected during tumor proliferation.	25
Figure 3: A schematic showing the step by step process of the overall system	28
Figure 4: Polyaniline structure	40
Figure 5: Polypyrrole structure.	41
Figure 6: Example of a complex architecture that can be obtain by the SAM technique. Image source [116]	43
Figure 7: The mushroom assembly	44
Figure 8: A black-box diagram showing the functions of the device.	59
Figure 9: Mushroom design.	64
Figure 10: CNT Towers design.	65
Figure 11: CNT Bed design.	65
Figure 12: Smart Polymer design.	66
Figure 13: Single Layer design.	66
Figure 14: Bilayer design.	67
Figure 15: Tri-layer design.	67
Figure 16: Single Layer with Surface Indentations.	68
Figure 17: Nanovelcro design.	68
Figure 18: One Enzyme Mushroom design.	69
Figure 19: One Enzyme Single Layer design.	69
Figure 20: One enzyme bilayer design.	70
Figure 21: Summary of the approach that was followed in this project in order to choose and optimize the design.	77
Figure 22: PPy electrochemical film deposition set up.	81
Figure 23: Set up of the lactate amperometry	84
Figure 24: Contact angles of a (A) clean electrode and a (B) PPy film embedded with LOx. The first image shows a hydrophobic surface while the second is more hydrophilic.	87
Figure 25: Change in system output over time after biosensor submersion in various concentrations of lactate. Averages of n=3 are displayed. As the system output increases, the lactate concentration increases proportionally.	89



Figure 26: The increase in system response is directly proportional to increase in current. ....89

Figure 27: Real-time recognition of increasing lactate concentrations via stepwise addition. There is an instantaneous response in the output response of the system as the concentration increases. Averages of n=3 are shown. ....90

Figure 28: Cyclic voltammetry results show about a 500% increase in the working area of the biosensor compared to a clean electrode.....88

Figure 29: The graph above shows the curve of lactate concentration in media vs. cell density. ....91

# Table of Tables

Table 1: The normal vs. abnormal extracellular baseline concentrations in rat glioma [25]. The baseline concentrations were taken from a different source measured in rat extracellular space [26].	26
Table 2: The normal vs. abnormal extracellular baseline concentrations for glutamate in rat glioma [25].	27
Table 3: Systemic concentration levels of metabolites in healthy vs. malignant tissue of rats [25]...	61
Table 4: Evaluation of the 12 designs based on the project objectives.....	73
Table 5: Summary of hypothesis that were taken into consideration when determining the parameters for the final designs. ....	78
Table 6: Summary of the parameters for the construction of the final designs. This chart is broken down based on the steps shown in Fig.21.....	78
Table 7: Contact Angle Analysis Results. ....	87
Table 8: The table below displays the lactate concentrations obtained using the biosensor in media from various cell densities.....	91

## **Authorship**

All team members contributed equally to all sections included in the report.

## Acknowledgements

The authors of this study would like to thank the following individuals:

- Professors Anjana Jain in the Biomedical Engineering Department and Professor Susan Zhou in the Chemical Engineering Department for advising the project.
- Yuan Yin of the Jain Lab for his immense support with understanding all lab protocols and always being available to help the team.
- Dina Rassias of the Jain Lab for helping when the team encountered difficulties.
- Zanzan Zhu of the Zhou lab for assisting in understanding of the signal processing equipment.
- Marie Tupaj of the Lambert Lab for providing help in contact angle experiments.
- Kathleen Wang and Mary Schwartz of the Camesano Lab for assistance with Atomic Force Microscopy.
- Lisa Wall for being a great resource for all logistical aspects of our project.

## Abstract

Implantable biosensors allow for continuous, real-time measuring of analyte concentrations and therefore show promise in monitoring the treatment of glioblastoma, the most aggressive form of brain cancer. Here, a biosensor system is presented as a glassy carbon electrode coated with lactate oxidase immobilized in a polypyrrole film. A prototype of the system was validated through benchtop and *in vitro* testing. The data showed that the system is sensitive in the physiological range and is over 94% accurate in real-time detection of subtle concentration changes of lactate produced from only 250,000 cells. This shows an improvement over current monitoring methods, which need differences on the magnitude of millions of cells in order to accurately detect tumor response.

# **Chapter 1**

## **Introduction**

## 1.1 Background

Glioblastoma multiforme (GBM) is a very aggressive and recurring stage IV astrocytoma [1]. It is the most common form of malignant glioma, resulting in an overall survival rate of 42.4% six months post-diagnosis with only 3.3% of all diagnosed patients surviving longer than two years [2]. This rate of survival persists even as cutting edge treatment technologies including surgery, radiotherapy, and chemotherapy, become increasingly advanced. Because time is a limiting factor, there is a high need for the ability to quickly and accurately monitor the patient's response to therapy. One developing technology that offers promise in this area is implantable, real-time, continuously-monitoring biosensors. A biosensor is an analytical device, which measures analytes by converting a biological response into an electrical signal [3]. Distinct differences in metabolic processes in malignant tissues cause an overexpression of certain metabolites when compared to healthy tissues [4], which can be measured using a biosensor. The mechanism of a biosensor can be broken down into three discrete steps: (1) biological recognition, (2) transduction into an electrical signal, and (3) processing of the electrical signal [3].

## 1.2 Design

This project focuses on detecting the overexpression of lactic acid in GBM using a biosensor system composed of lactate oxidase (LOx), horseradish peroxidase (HRP), polypyrrole (PPy), chitosan (CHI) and a glassy carbon electrode as shown in Figure 1. The

[1] Zhang, X., et al. (2012) *J Exp Ther Med.* 3(1): p. 9-14.

[2] Reardon, D.A., et al. (2006) *J Clin Oncol.* 24(8): p. 1253-65.

[3] Zhang, S., et al. (2000) *Biosens Bioelectron.* 15(5-6): p. 273-82.

[4] Gatenby, R.A., et al. (2004) *Nat Rev Cancer.* 4(11): p. 891-9.

biocompatible PPy film serves to immobilize the LOx and to aid in the conduction of generated electrons. The chitosan layer serves to keep electroactive particles from interfering with the current level. LOx was chosen due to its ability to selectively bind to lactic acid and convert it into hydrogen peroxide ( $H_2O_2$ ).  $H_2O_2$  is further broken down into free electrons in the presence of HRP. These free electrons are measured as a current level using a reference and working electrode and compared to established metabolic levels. The goal of these approaches is to optimize the sensing capabilities of biosensors, such as sensitivity, stability, biocompatibility, reproducibility, and selectivity for monitoring GBM.

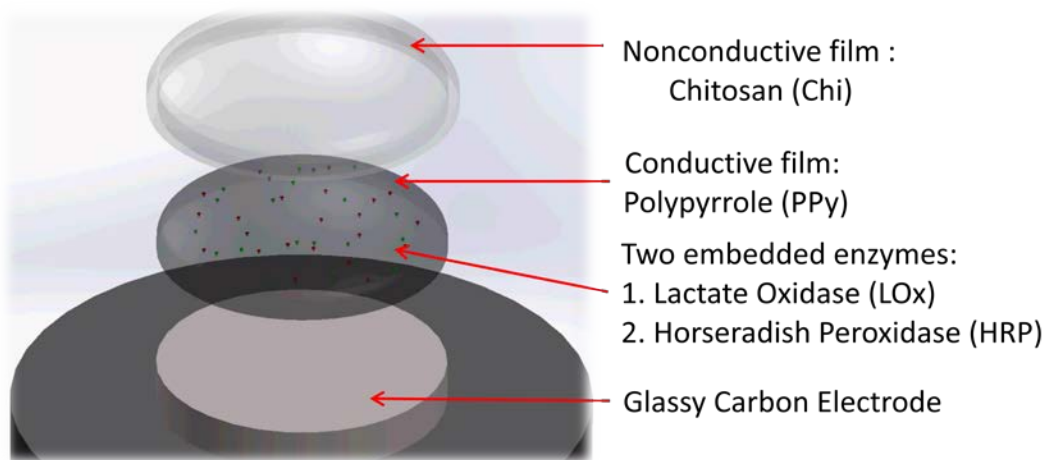


**Figure 1. Overview of the design.**

### **1.3 Methodology for Prototype Development and Validation**

For the preliminary validation of the concept behind the design, bottom-up method was followed. The testing performed in this project was done with a simplified design shown in Figure 2, consisting only of a PPy layer with LOx enzyme, omitting the CHI layer and HRP enzyme.



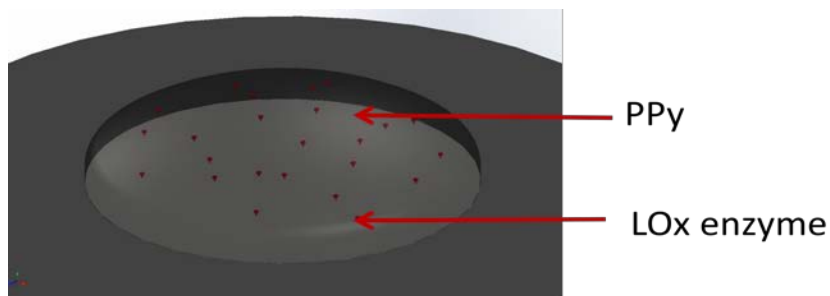


**Figure 2. Preliminary prototype design for validation of the system.**

A polished and cleaned glassy carbon electrode (GCE) was modified using an electrochemical deposition method. The GCE electrode and a AgCl reference electrode were placed in a degassed solution of PPy and LOx suspended in KCl buffer and were subjected to a constant current for a specific duration using the GPES software and the AUTOLAB potentiostat (Metrohm). Tests were performed on the GCE to characterize its properties and validate deposition. Contact angle analysis was conducted by dispensing 2 $\mu$ L of water on the surface of the electrode and the contact angle of each side of the drop was measured and averaged using the software.

Several tests were then performed with the GPES software and AUTOLAB system with freshly-deposited PPy films containing LOx. A lactate amperometry test was conducted to validate the presence of LOx enzyme. A constant voltage was applied while the modified electrode was submerged in each of the following lactic acid concentrations 1000 $\mu$ M, 500 $\mu$ M, 100 $\mu$ M, and 500nM and the current response was measured over time. A real-time lactate recognition test was conducted with a modified electrode in a beaker of PBS where 1mL drops of lactic acid concentrations ranging from 10mM-1M were added every 60s. Lastly, cyclic voltammetry was performed on clean electrodes and electrodes modified with PPy to determine the conductivity of the film. Lastly, an *in vitro* test was performed to validate the system in physiologically similar conditions. A commercial

colorimetric Lactate Assay kit (Sigma Aldrich) was used to analyze the lactate concentration in media obtained from a culture of 1.25 million astrocytoma cells (U87mg) and another culture of 1.5 million. The level of lactate in the media was then measured using the biosensor system. The values were compared in order to determine the

#### **1.4 Results**

The results of the contact angle analysis indicate that the deposited PPy film has an average contact angle of  $41.6^\circ \pm 8.4$ . The clean electrode, which served as a control, has a contact angle of  $85^\circ \pm 4.1$ . The lactate amperometry show that the 500nM concentration of lactate exhibits the smallest decrease in current and 1000 $\mu$ M exhibits the largest decrease. The results of the real-time recognition test indicate that as the concentration of lactate increases, there is an instantaneous response in which the current increases proportionally in negativity. Cyclic voltammetry showed that the PPy film caused no significant impedance in the transfer of electrons to the electrode surface, exhibited by a  $1.5 \cdot 10^{-5}$ A change in the reduction point and a  $3 \cdot 10^{-5}$ A in the oxidation point, as displayed in Figure 3. The *in vitro* tests validated that the sensitivity of the system is in the nanometer scale which is relevant in the physiological conditions and that the accuracy of the system was over 94% in detecting the change of lactate levels produced by a change in cell number of 250000 cells.

#### **1.5 Discussion**

In this project, we were able to design, develop, and validate an enzymatic biosensor system that can detect differences in metabolite levels. This allows for the application of the system to monitor GBM. Our biosensor allows for real-time measurement and sensitivity in the nM range while remaining reproducible and simple to manufacture. In

future design iterations, a CHI layer will be incorporated in order to decrease interference from electroactive particles, allowing for a more reliable device under *in vivo* conditions. Additionally, HRP, which quickly breaks down  $H_2O_2$  into free electrons, will be added to the PPy film to decrease response time as well as increase the sensitivity of the system. In order to better monitor GBM, a second working electrode that detects glutamate changes using glutamate oxidase will be added to the system. In parallel, the system will be optimized for *in vivo* implantation through miniaturization of the electrode components.

# **Chapter 2**

## **Background and Literature Review**

## 2.1 Introduction

Approximately 17,000 people are diagnosed with brain tumors each year in the United States alone, with 13,000 associated annual deaths [1]. The most prevalent form of brain tumors is glioma [2], which account for 70% of all brain tumors [3]. There are two main types of gliomas: astrocytomas and oligodendrogliomas, which can be further characterized by grade and location [4]. Astrocytomas are the most common type of gliomas [3]. Stage IV astrocytoma, its most aggressive form, is also known as glioblastoma multiforme (GBM) and it is the most prevalent form of all brain tumors [5]. Despite the advancements of modern day therapeutics, the survival rate of patients with GBM is very low, with less than 2% of all patients surviving past the first three years [6]. Figure 3, shows the distribution of rates of survival over the first two years after initial diagnosis [7].

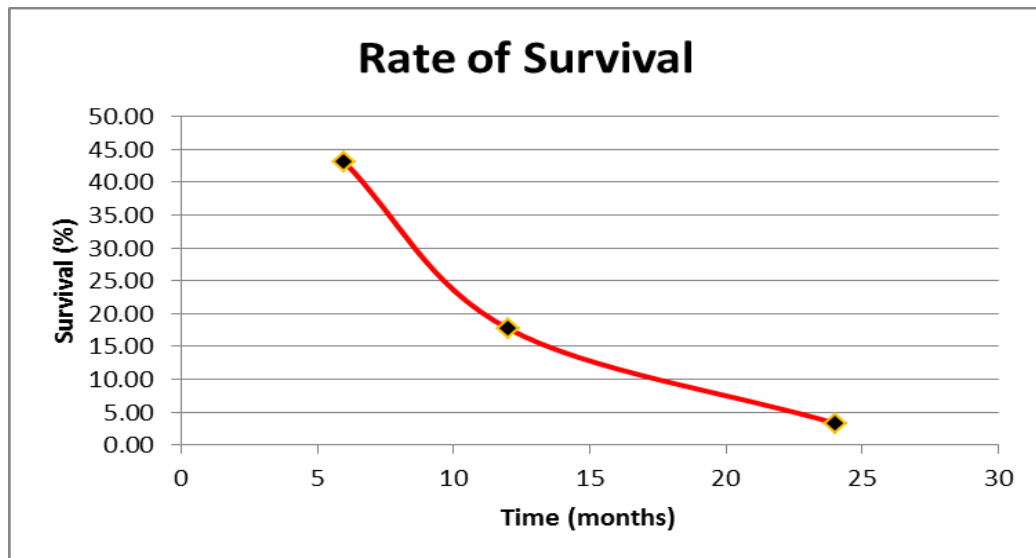


**Figure 3: Survival rate of patients within two years after diagnosis.**

One of the main factors that contribute to low survival rate is the lack of evident symptoms [8]. Patients do not undergo testing for GBM until they exhibit symptoms such as dizziness, severe headaches, or blurry vision [8]. These symptoms can at first appear trivial

and can be overlooked, or misdiagnosed, causing accurate diagnosis to occur only after GBM has progressed significantly in most patients.

Magnetic Resonance Imaging (MRI) and Computed Tomography (CT) scans are currently used for the detection of GBM. While these technologies are useful, they both have several limitations. MRI is a device that uses a varying magnetic field to map the hydrogen content in the body to produce an image. MRI scans are advantageous for imaging soft tissues due to the high concentration of hydrogen within these soft tissues. When a proton comes in contact with a magnetic field, they will align themselves in the direction of the field [9]. The data is reconstructed into a 2D illustration, with a darker image for dense tissue and lighter image for tissues that contain more water [9]. However, when imaging brain tumors, if the tumor is too small the MRI may not be able to detect it due to low concentration of hydrogen molecules, thus making it difficult for the doctor to distinguish between cancerous and healthy cells [10].

CT is a device that uses X-rays to generate 3D images of the body's internal organs. X-ray tubes rotate around the patient and measure the number of photons that are able to get through the tissue. CT scans are widely available and they provide 3D images of tissues, which lack distortion found in 2D images of MRI, however CT scans are harmful to the patient as the radiation can damage DNA. CTs also lack contrast between soft tissue and tumors which can lead to misdiagnosis [11].

After the patient is diagnosed with a brain tumor, determining the most effective treatment depends on the size and progression of the cancer. Once the cancer has progressed to a life-threatening status, the only option is to immediately perform surgery to remove the tumor [12]. This is a delicate and risky procedure due to its invasiveness.

However, if the cancer is detected at an early stage, surgery can be avoided. Instead, other treatment types can be used to kill the cancer cells or to control the proliferation rates. The second type of treatment is chemotherapy which involves the use of drugs to kill cancer cells by inducing apoptosis (self-programmed cell death). However, most drugs cannot diffuse across the blood brain barrier and require very precise dosage control to be effective while causing minimal side effects [12]. The third treatment technique, radiation, eradicates malignant cells by targeting tDNA [13]. Radiation therapy is used after surgery as protective measure against recurrence and it is a common practice to combine chemotherapy with radiotherapy [13]. One of the drawbacks of using radiotherapy is that not only does it damage the DNA of cancer cells but also the DNA of healthy cells [14].

A better diagnostic and monitoring system is needed in order to combat the aggressiveness of GBM so that patient survival rates can be increased. Even though both MRI and CT scans are used globally, they have some significant disadvantages including poor resolution as well exposing the patient to radiation. Finding new technologies to perform these functions is imperative.

## 2.2 Biology of Cancer

### 2.2.1 Cell Metabolism

Normal differentiated cells rely on the production of energy from cellular respiration in order to fuel normal cell activity. Cellular respiration entails a number of metabolic processes that convert biochemical molecules, such as glucose, into a usable form of energy. In the presence of oxygen, normal cells primarily metabolize glucose into pyruvate through glycolysis for growth and survival. This is generally followed by complete mitochondrial oxidative phosphorylation of the pyruvate in the Krebs cycle, which generates 36 ATP molecules per molecule of glucose [15]. When there is no oxygen present, normal cells still convert glucose to pyruvate through glycolysis, but pyruvate is then converted to lactate through a process called anaerobic glycolysis. The process of anaerobic glycolysis produces only 2 ATP molecules per glucose, presenting a method that is extremely inefficient compared to normal oxidative phosphorylation [16]. Mitochondrial oxidative phosphorylation is also observed in astrocytes in the brain [17].

Astrocytes are the most abundant cell type in the central nervous system [CNS] and are mainly responsible for maintaining normal extracellular amino acid concentrations. The most notable amino acid that astrocytes regulate is glutamate, which is the major excitatory neurotransmitter in the CNS [18]. It is known that glutamate is released as a synaptic transmitter in the brain it is immediately taken up by surrounding astrocytes and metabolized into glutamine, a non-neuroexcitatory amino acid, which is then transferred back to neurons for reconversion to glutamate This is referred to as the glutamate-glutamine cycle in the brain [18].

Normal brain function depends critically on an adequate energy supply in the form of oxygen and glucose provided by the blood. ATP is almost entirely generated by normal



cellular respiration processes as mentioned above. Oxidative phosphorylation produces approximately 87% of ATP in the brain, about 26-30 molecules of ATP [19]. Typically, neurons in the brain regulate the energy supply by switching on glycolysis in astrocytes. When active neurons release glutamate, it is taken up into astrocytes, initiating the glutamate-glutamine cycle, which is powered by the generated ATP from oxidative phosphorylation. ATP is necessary to keep the glutamate-glutamine cycle moving in order to closely regulate the extracellular concentration of glutamate in order to avoid neurotoxic effects that can lead to necrosis [19].

### **2.2.2 Role of Altered Cell Metabolism in Cancer**

Cancer is a disease that is caused by a series of genetic mutations or alterations within the genes of cells. These mutations affect specific genes that are responsible for regulating cell proliferation rates and inducing cell death [20]. These mutations can be inherited or can be caused by hazardous environmental factors that damage the cell's DNA. As previously mentioned, in normal cell differentiation, cells are created and destroyed as needed. Mutations can override normal cell function causing abnormal cells to not only proliferate at an uncontrollable rate, but also extend their lifetime. As a result of uncontrolled cell proliferation, large biomasses or tumors form and energy demands of cell increase in order to keep up with the rapid growth [20].

When abnormal cells are proliferating, normal cell metabolism no longer fulfills the needs of these cells to survive. Therefore, the metabolism of cancer cells is adapted to facilitate one main function, the uptake and incorporation of nutrients [15]. This switch in cellular metabolism has been termed the Warburg effect, which states that cancer cells rely on aerobic glycolysis to generate the energy needed [21]. Aerobic glycolysis is an inefficient

method to generate ATP since it only yields 2 molecules per unit of glucose. The energy needs of the cancer cells are much higher than what aerobic glycolysis can provide [22]. Figure 1 illustrates the major metabolic switches that occur in normal tissue compared to proliferative tissue or tumor cells. According to the figure, proliferative tissue converts 85% of consumed glucose into lactate as a result of the adaptation to aerobic glycolysis [15].

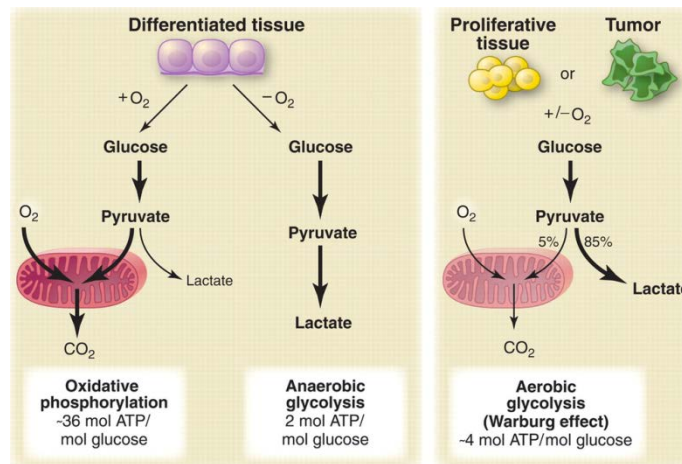


**Figure 4: Illustration highlighting the differences between oxidative phosphorylation, anaerobic glycolysis, and the Warburg effect through aerobic glycolysis [15].**

The exact reason cancer cells rely on such an inefficient cell metabolism such as aerobic glycolysis is unclear, but what is clear is that there are major changes exhibited by two major metabolic pathways during abnormal cellular respiration. The metabolism of glucose in the glycolic pathway exhibits an increased consumption of glucose to supply the energy needs of proliferative cells and an increased production of lactate as a result of tumor cells undergoing aerobic glycolysis. The second metabolic pathway that is affected is the metabolism of the amino acid glutamine, this metabolic reaction is known as glutaminolysis [23]. Glutamine provides cells with the necessary carbon and nitrogen vital for growth. During rapid proliferation the abnormal cells require higher levels of glutamine

to support those functions. As a result of this increased glutamine consumption, there is an increased production of lactate and alanine, the products of glutaminolysis [24]. Figure 2 provides a hierarchical chart breaking down the pathways and metabolites affected during tumor proliferation.

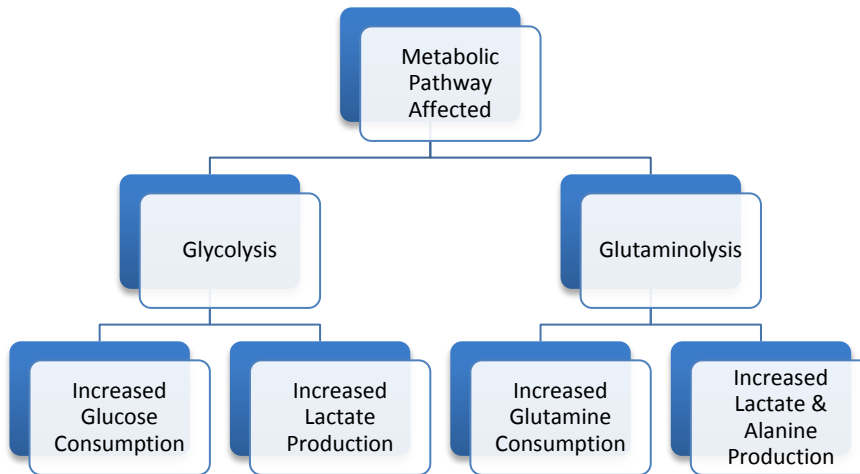


**Figure 5: Above is a hierarchical illustration of the metabolic pathways and specific metabolites affected during tumor proliferation.**

There are a number of metabolites that are affected but the most notable are the ones on the last level of the hierarchical chart. Below in Table 1, the normal extracellular baseline concentrations compared to the abnormal extracellular baseline concentrations are displayed for each of the specific metabolites known to be affected in these two metabolic pathways.

**Table 1: The normal vs. abnormal extracellular baseline concentrations in rat glioma [25]. The baseline concentrations were taken from a different source measured in rat extracellular space [26].**

	Normal extracellular baseline concentrations ( $\mu\text{M}$ )	Abnormal extracellular baseline concentrations ( $\mu\text{M}$ )
Glucose	200 $\pm$ 30	160.9 $\pm$ 76.2
Lactate	400 $\pm$ 50	301.1 $\pm$ 57.2
Glutamine	28.7 $\pm$ 2.37	29.56 $\pm$ 4.23
Aniline	4.58 $\pm$ .97	10.28 $\pm$ 13.2

### 2.2.3 Cell Metabolism of Glioblastoma Multiforme

When genetic mutations within the genes of astrocytes occur, these cells take on the same behavior observed by most cancer cells. These diseased cells proliferate rapidly and uncontrollably, greatly increasing the number of malignant cells in the area. This significantly alters the normal metabolic needs of the cell, resulting in the creation of a biomass referred to as an astrocytoma. Astrocyte differentiation undergoes a switch to a metabolism driven by aerobic glycolysis, which is the Warburg effect. When the astrocytes implement the inefficient generation of energy, a number of things occur. As with cancer cells in general, there is an increase in consumption and production of a number of metabolites such as glucose, alanine, and lactate to fulfill the needs of proliferative astrocytes [25]. Previous studies show that there is another metabolite affected specific to astrocyte metabolite changes. In GBM, glutamate uptake is decreased compared to normal astrocytes. Normal astrocytes rapidly deplete glutamate as it is released from active

neurons with the help of the ATP driven glutamate-glutamine cycle. Since astrocytes are now producing less ATP, the glutamate is no longer being transformed, and therefore it is accumulating in the extracellular space of the brain, raising the baseline concentration of this metabolite [18]. Table 2 displays the normal extracellular baseline levels of glutamate in the brain compared to the reported elevated levels of glutamate as a result of this metabolic switch.

The change of glutamate is specific to the astrocyte altered metabolism and it is in addition to the previous mentioned metabolite changes common to all cancer. Due to the drastic changes in metabolite concentrations of glucose, lactate, alanine, and glutamate between normal and abnormal astrocytes, analyzing these changes offers a novel way to monitor the progression of GBM.

**Table 2: The normal vs. abnormal extracellular baseline concentrations for glutamate in rat glioma [25].**

	Normal Extracellular Baseline Concentrations ( $\mu\text{M}$ )	Abnormal Extracellular Baseline Concentrations ( $\mu\text{M}$ )
Glutamate	$1.12 \pm 0.3$	$2.61 \pm 1.75$

## 2.3 Biosensors

A biosensor is an analytical device, which measures analytes by converting a biological response into an electrical signal (IUPAC). An analyte can be any biological molecule such as DNA, ligands, or metabolites. The mechanism of a biosensor can be broken down into three discrete steps and can be seen below in Figure 3:

- 1) Biological recognition
- 2) Transduction into an electrical signal
- 3) Processing of the electrical signal.

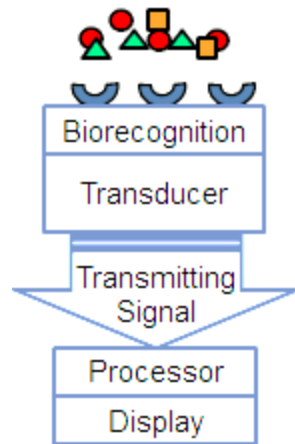


**Figure 6: A schematic showing the step by step process of the overall system**

The biosensor will recognize and bond to the metabolite of interest. This reaction will convert or transduce the biological response to an electrical signal, which is transmitted to the processor via the electrode. The processor correlates and displays a visual representation of the generated data. These three steps can be performed through different mechanisms, such as using an optical, thermal, or electrochemical approach [26].

### 2.3.1 History of Biosensors

Biosensors emerged in the 1960's from the need to monitor glucose levels in diabetic patients [27]. Biosensor research can be categorized into three distinct

generations since Lyon and Clark's first initial research. Each new generation of biosensors focuses on a fundamental change in the method by which electrons are carried from the site of transduction to the electrode. The first generation pioneered by Clark and Lyons used natural mediators such as oxygen in the blood to carry the electrons [28]. In the second generation, synthetic mediators were developed in order to increase the efficiency of this process. In third generation research, which is still being conducted, the mediators are eliminated. These biosensors rely on direct electron transfer (DET) from the active biological transduction site to the electrode to increase the efficiency of the monitoring ability. The most efficient way to achieve DET would be to place the biological agent directly on the surface of the electrode; however, this would result in reduced biological activity [29]. Therefore, most third generation research focuses on creating a more electrically conductive environment to help transfer the free electrons to the electrode. This is performed by placing an intermediate material between the biological agent and the electrode.

Intermediate materials can be categorized into two types of electrode coatings: films and nanostructures. Films can consist of materials that are conductive (i.e. graphene and polyelectrolytes), non-conductive (i.e. chitosan and alginate), or a combination of both materials [29]. Nanostructures currently being used in research include carbon nanotubes and nanoparticles consisting of materials such as gold or silver. Newer approaches focus on developing composites of films and nanostructures [30]. The goal of these approaches is to optimize the sensing capabilities of biosensors, such as sensitivity, stability, biocompatibility, reproducibility, and selectivity.

### **2.3.2 Current Applications**

Biosensors are currently receiving a tremendous amount of attention because the technology offers the possibility for simple, inexpensive, accurate and sensitive platforms for patient diagnosis [26]. The market for biosensor applications is expanding as biosensor capabilities such as sensitivity and selectivity improve. Glucose biosensors currently make up the largest market presence [28]. Some main contributing factors to their market dominance include the increasing population of diabetic patients and urgent need for accurate and user compliant devices to meet the rising number of point-of-care applications. There are still major challenges in achieving clinically accurate, continuous glucose monitoring, however this remains one of the most developed applications of biosensors [28].

Since Clark and Lyons initial development of glucose biosensors, the design of these devices has evolved a great deal. Currently, simple non-invasive glucose biosensors can be bought and used at home. No other application has experienced this evolution in design over the past 50 years. This phenomenon is due to the considerable research that has, and is, being conducted in order to enhance the sensing capabilities of biosensors at the expense of expanding biosensor applications.

### **2.3.3 Design Criteria**

Currently, biosensor research is aimed at enhancing the sensing capabilities of third generation biosensor technology. Third generation biosensors can differ in the fundamental way that they operate, with amperometric, potentiometric, impedimetric, and optical electrodes all providing methods to sense concentrations of biomolecules. However, amperometric electrochemical electrodes are receiving widespread attention and use due to their simplicity, fast response times, and sensitivity to a wide range of



biomolecules [31-33]. These biosensors operate on applying a base current between a working electrode and reference electrode, with the reduction or oxidation of a compound causing a shift in the current allowing for quantification of specific molecules [34]. Methods to enhance the selectivity, response time, sensitivity, signal to noise ratio, and stability as well as decrease biofouling and interference associated with these biosensors are being developed. In some cases, improvements in one sensing area can inhibit another area, highlighting one of the difficulties facing researchers as they attempt to enhance these capabilities.

#### 2.3.3.1 Selectivity

The selectivity of biosensors is the ability of the device to monitor only one analyte out of a vast variety of possible analytes in a physiological environment [33]. This means that the biosensor must be able to selectively recognize the analyte of choice. For amperometric biosensors, enzymes – and more specifically oxidase enzymes - are widely used for this biorecognition since they are the most selective agent and exhibit good stability [35]. Enzymes have the ability to react with a single substrate, fulfilling the biorecognition element of biosensors. Oxidase enzymes serve to break down the target molecule into products that contain hydrogen peroxide. This hydrogen peroxide is then oxidized by the current applied to the working electrode [36]. For this reason, a voltage high enough to perform this function is needed, which can serve to oxidize other molecules in the area of the electrode such as acetaminophen or ascorbate [37]. This causes an increased electrical signal to be conducted through the electrode, providing false readouts of analyte concentrations. The ability to reduce the current applied to the working electrode is necessary, with some novel approaches being developed to do so. By designing

bienzymatic devices that consist of the original bioselective enzyme and another peroxidase enzyme, the hydrogen peroxide does not need to be oxidized by the current to be transduced into an electrical signal, allowing for a large decrease in the potential applied to the working electrode [31, 36, 38, 39]. Traditionally, horseradish peroxidase enzymes have been used for this purpose, but more recently other peroxidase enzymes such as sweet potato peroxidase have been utilized with similar results [31].

Additionally, by reducing the ability of interfering molecules to reach the electrode, the selectivity of the biosensor can also be increased. This is typically performed by the addition of a membrane as the outer layer of the biosensor. The use of materials that can provide size exclusion is one method. The precise control over pore size would allow any molecule larger than the analyte of choice to reach the oxidizing area of the electrode. This method has shown effective in pyruvate biosensors, which show exclusion of ascorbate when placed in dialysis tubing [40]. This size exclusion method of increasing selectivity can be enhanced further by combining it with anionic exclusion. The electropolymerization of pyrrole and o-phenylenediamine has been shown to achieve a very high selectivity using this method [41, 42]. The only drawback to using membranes to increase selectivity is the effect it has on decreasing the temporal resolution of the device [37].

### **2.3.3.2 Sensitivity**

Sensitivity refers to the concentration level at which the biosensor can sense the analyte of interest (micromolar, millimolar, etc.), and the desired sensitivity is dependent on the analyte itself. For instance, if glucose was to be monitored in humans, a sensitivity on the millimolar (mM) scale would be necessary, but if glutamate were to be monitored a sensitivity on the micro or nanomolar (nM) scale would be desired [37]. One way in which

the sensitivity of the biosensor can be easily increased is to increase the applied current to the working electrode. This serves to more easily oxidize the metabolite of interest in the environment. However, this increase comes at a significant cost of selectivity, since the increased current can serve to oxidize a wider range of biomolecules in the area of the working electrode. For this reason, other methods have been undertaken to increase the sensitivity. One major development to this end is to platinize the surface of the electrode [40, 43]. Adding a layer of platinum to the electrode increases the surface area of it, and therefore leads to a greatly increased sensitivity.

Another approach used to increase the sensitivity of the electrode is to use different electrode materials. Different materials, such as carbon, gold, platinum, and palladium, have different physical and electrical properties that can play a role in the choice of electrode. For instance, platinum (as seen with the platinizing layer) exhibits the highest sensitivity [33]. However, its ease of desposition is low, which may limit its use [36]. Palladium, gold, and glassy carbon are, in order, the next highest ranking in sensitivity. These materials exhibit a much higher overpotential, around 4-5 times higher, in order to oxidize hydrogen peroxide[33]. However, glassy carbon is widely used as a material in order to create inexpensive and disposable biosensors [38].

The newest, and most promising, approach to increasing the sensitivity of biosensors is the introduction of nanomaterials into the design. Nanomaterials can have two effects when used to modify the surface of the working electrode: to increase surface area and to increase conductivity. For example, nanoparticles consisting of gold, platinum, and silver have been deposited to increase surface area of the working electrode [44-46]. The most promising of the nanostructures currently being researched are carbon

nanotubes. These structures can be single walled or multiwalled, and a significant amount of research has been conducted to characterize them. When used in biosensors, they can be highly aligned and spaced in order to act as nanoelectrodes that pervade the biosensor structure and impart a very high sensitivity [33].

### **2.3.3.3 Stability**

In order for an implantable biosensor to be of any use, it must accurately report concentrations of the analyte of interest for an extended period of time. This means that the device must exist in physiological conditions for weeks or months to perform its designed function. The main factor responsible for low stability is loss of activity of the biorecognition element [32]. This decrease in activity can be attributed to denaturation as a result of changes in pH, temperature, etc. or proteases degrading the biorecognition element. Therefore, to ensure long-term stability of the device, it is necessary to maintain ideal local conditions for the biorecognition element as well as prevent infiltration of degradation enzymes into the biosensor area. These two criteria are commonly fulfilled through the use of an outer protective membrane. The properties of the membrane can be tailored in order to keep any biological agent that can induce denaturation or degradation of the recognition element out to increase stability.

Another factor that can greatly affect the biorecognition agent's activity is the method used to fix the agent in place in the biosensor [32]. There are currently hundreds of protocols outlining methods to immobilize biorecognition agents, but many serve to decrease stability of the molecule. When immobilizing an enzyme, the pH, temperature, reaction time, rigidity, etc all need to be accounted for in order to optimize the immobilization with regards to long term stability [47].

Currently, the average time that a device has retained 100% stability, as seen in the literature, is 21 days [48-50]. Most of these devices retain complete, or nearly complete, stability for the 21 days, and experience a slight to moderate decrease afterwards. One of the best rates of stability seen was with a glucose biosensor based on graphene that retained 80% stability for up to 50 days [50].

#### **2.3.3.4 Biofouling**

An important characteristic to control with respect to biosensors is biofouling. This is the accumulation of biological materials, such as proteins and cells, on the surface of the device [51]. This accumulation can lead to complete failure of the device by fibrous encapsulation which completely impedes the ability of the analyte of interest from entering the biosensor environment [51]. Reduction in biofouling is entirely dependent on the contact surface of the biosensor, since this is what biological materials can sense. A commonly used design approach to decreasing biofouling is to add an outer membrane to the biosensor. This allows for the outer surface to be selectively modified to decrease protein adsorption, the first step in biofouling [51]. Membranes can be naturally derived (silk, collagen, etc) or synthetic (pluronic, polyethylene glycol, etc) and attempt to either decrease all biological interactions or promote desirable interactions. Although a surface that causes no biofouling may not be possible, diminishing the biofouling effects to extend biosensor stability is a necessary consideration in implantable biosensors.

#### **2.3.3.5 Response Time**

Response time in biosensors is characterized as the time taken to reach a steady-state readout of analyte concentration [34]. The steady state response time is defined as the time it takes to reach 90% of this steady-state response [52]. This property of the

biosensor is dependent on the analyte of choice, the ability of it to diffuse through the various layers incorporated in the biosensor, and the activity of the biorecognition element [34]. Ideally, a biosensor would provide information on analyte concentration levels as instantaneously as possible in order to provide real time monitoring capabilities. Depending on the application of the biosensor, different response times are necessary. Response times on the scale of microseconds may be necessary for applications that include monitoring sub second biological interactions, but a response time on the level of seconds would be appropriate for other applications such as glucose monitoring. Therefore, it is imperative to weigh the needs of the biosensor when deciding if response time is the characteristic that is necessary to optimize, since it often can come at a cost of other sensing capabilities.

#### **2.3.3.6 Sensing Capability Tradeoff**

As it can be seen, the various sensing capabilities often have an inverse relationship with each other. Adding a membrane to increase selectivity will decrease response time. Decreasing the applied voltage to the working electrode to increase selectivity will subsequently decrease the sensitivity of the biosensor. Removing a membrane to increase the response time may increase the biofouling of the device. Therefore, when designing a biosensor it is of utmost importance to account for the effect of a single change on all of the sensing capabilities that the biosensor will ideally have. Otherwise, small changes in design can lead to failure of the design to optimally perform its functions.

#### **2.3.4 Biosensor Coatings**

Recently, a significant amount of research in the field of biosensors has been focused on enhancing sensing capabilities with the use of electrode coatings for the immobilization

of the biorecognition component and this approach has shown several advantages. The presence of a coating can minimize access of compounds to the surface of the electrode which increases the sensor's selectivity by decreasing its interference [53] [54]. A coating can minimize access to other electroactive particles that may be present in the body, such as ascorbate or acetaminophen [37, 53]. Applying a coating also serves the role of a transport-limiting component. Enzymatic biosensors operate based on a flux of substrate towards the enzyme. Depending on the level of substrate, in order to maintain balance with reaction kinetics, it is necessary to limit the transport of substrate, to ensure that the enzyme is free for binding [55, 56].

Furthermore, a coating around the electrode can also serve to improve the stability of the encapsulated biocomponent. One of the biggest issues with early biosensor technology was the loss of activity of the biorecognition molecules over time [53, 57, 58]. Enzymes in particular are known to denature when exposed to the metallic electrode [58]. This not only lowers the selectivity of the biosensor by lowering its biorecognition, but it can also result in the buildup of a layer around the electrode that prevents the transport of electron [53].

Lastly, another major function of utilizing coatings around the electrode is the improvement of biocompatibility. The hydrophobic outer layer of the naked electrodes leads to biofouling: the collection of serum proteins on the surface of the electrode, which creates a "road-block", or a physical interference, for the analytes and thus impedes the measuring capabilities of the biosensor [37, 51, 53, 54, 56, 59]. Depending on the biosensor implantation site, a lipid layer may also form around the electrode to create a hydrophobic

capsule that blocks analytes out. The use of a coating with hydrophilic properties can significantly reduce the level of biofouling [37, 53, 54, 56].

With the addition of a coating onto the electrode, it is necessary to take into consideration the level of diffusion of particles through the films. This parameter is described by Fick's 1<sup>st</sup> law of diffusion shown in Equation 1, where  $D$  is the diffusion coefficient,  $C$  is the analyte concentration,  $C_0$  is the initial concentration,  $l$  is the distance around the film, and  $L$  is the thickness of the nanofilm [56].

$$D = \frac{dC}{dt} * \frac{lL}{C_0}$$

**Equation 1.**

This equation states that the number of moles of an analyte transported across a thin film per unit of time is equal to the product of the flux and the area across which the transport is taking place. This equation can be used in the design of coatings to estimate the diffusion parameters of a coating [56].

Polymers have led the way as electrode coatings due to their ability to improve on the issues summarized above, as well as due to their light weight, low cost, ease of production and processing, flexibility etc. [53, 54, 60]. Two categories of polymers have been extensively utilized in the field of biosensors: non-conductive and conductive polymers.

#### **2.3.4.1 Conductive Films**

Polymers are generally thought of as insulating materials, however in the late 70s Shirakawa and his colleagues discovered that acetylene, a non-metal, exhibited high conductivity when exposed to chlorine, bromine or iodine vapors [61]. This technique was



later termed as doping, and it has been utilized to turn many polymers into conductive materials, including poly(pyrrole)s, poly(thiophene)s, poly(terthiophene)s, poly(aniline)s, poly(fluorine)s, poly(3-alkylthiophene)s, polytetrathiafulvalenes, polynaphthalenes, poly(phenylene sulfide), poly(phenylenevinylene)s, poly(3,4-ethylenedioxythiophene), polyparaphenylene, polyazulene, polyparaphenylene sulfide, polycarbazole, and polydiaminonaphthalene [54].

Conductive polymers are unique due to the fact that they have metallic and semiconductor characteristics. The reason they exhibit this behavior is the presence of alternating single and double bonds between carbon atoms in the backbone, each of which contains a strong “sigma bond” and a weaker “pi bond”, allowing for electron flow. When these materials are doped, in other words, when electrons are either added or removed from the material, the electrons located in the “pi bonds” are then free to move [54].

The use of these conductive polymers for medical applications has been limited by their biocompatibility, where only poly(pyrrole), poly(aniline) and poly(thiophene)s are biocompatible and thus can be incorporated in implantable devices [54, 60, 62-65]. Further limitations include difficulties in manufacturing and processing, which are particularly encountered with polythiophenes[60, 62, 65], therefore polypyrrole and polyaniline are considered to be the optimal choices in biosensor coatings [53].

#### **2.3.4.1.1 Polyaniline (PANI)**

PANI, shown in Figure 4, has been used extensively in biosensor research [54, 60, 62-67]. It exhibits relatively high conductivity in its doped state of up to 1S/cm [54]. The polymerization reaction can be easily controlled and it is inexpensive and thermally and electrochemically stable [54, 62, 67]. PANI can be made conductive by HCl doping, which

gives it good environmental and thermal stability [54]. However, processability and modification of PANI has been shown to be challenging [64-66]. To improve on this aspect, one technique that has been developed is the dispersion of PANI onto electrodes in the form of nanoparticles, instead of a complete layer of coating [63].

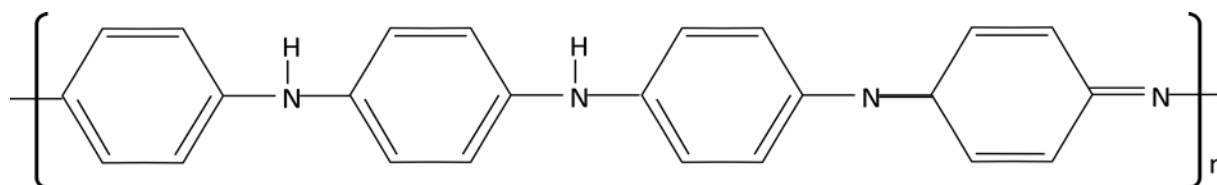


**Figure 7: Polyaniline structure**

#### **2.3.4.1.2 Polypyrrole (PPy)**

The structure of PPy is shown in Figure 5 Without hesitation, PPy is the most commonly used conductive polymer for biosensor applications [53]. Its conductivity can be up to 1000S/cm which is close to the conductivity of metals, due to the presence of polarons: positively charged defects [54]. PPy offers the best biocompatibility of all conductive polymers and best support for the immobilization of biocomponents [53]. One characteristic that distinguishes PPy from the previously aforementioned polymers is the fact that it is electroactive at the physiological pH of around 7[53, 54]. PANI and polythiophenes on the other hand require an acidic environment at deposition, which makes them more difficult to use for biological applications [53, 68, 69].

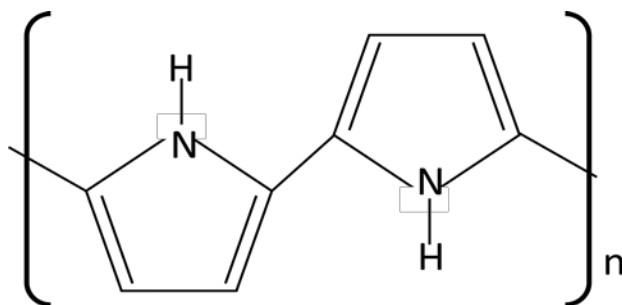


**Figure 8: Polypyrrole structure.**

#### 2.3.4.2 Non-conductive Coatings

The major advantage to non-conductive coatings is that they prevent adsorption of proteins, thus improving the biocompatibility of devices [53]. Non-conductive coatings generally have a thickness of 10-100nm, therefore they allow for the analytes and reaction product to diffuse rapidly [70, 71]. The non-conductive polymers that have found a vast use in the recent decade in biosensor technology are phenol-based, phenylenediamines (PPD), as well as over-oxidized PPy [70]. Synthetic ethylene-based polymers have also played a major role in this field with PEO/PEG as well as Pluronic [53, 72-74].

Along these synthetic polymers, natural polymers, mainly polysaccharides, have also received a great deal of attention in the research for biosensor enhancement, including agar [75] and alginate [76]. In particular, chitosan (CHI) has been vastly explored as a natural immobilization matrix [30, 77-84]. CHI is derived by the deacetylation of chitin and formed as a copolymer of glucosamine and N-acetylglucosamine with glucosidic bonds [83, 85]. CHI offers a combination of desirable properties: it has excellent film-forming ability, it is biocompatible, non-toxic, inexpensive, thermally and chemically inert, has good permeability, and good mechanical strength [86, 87]. It can also be easily modified because of its high number of amine groups which serve two functions when used in biosensors: (1) they allow for immobilization of enzymes by covalent bonding [88] and (2) can adsorb

metal ions to prevent enzyme damage [89, 90]. As can be seen, a variety of conducting and non-conductive coatings have been researched so far, with the goal of increasing biosensor performance by increasing its sensitivity and decreasing its interference, respectively.

#### **2.3.4.3 Multilayer Nanofilms**

With the extensive research that took place in biosensors enhancement, one approach developed involves the use of more than one coating layer on an electrode. There are two main techniques that have been used to create such assemblies: the Langmuir-Blodgett technique and self-assembling coatings.

The Langmuir-Blodgett technique is a very simple approach where the desired solid surface is briefly immersed in an amphiphilic solution, to obtain a one molecule-thick layer of the solution onto the surface [91-94]. While this technique allows for great control over the architecture of the films and improves the biosensor performance, the technique that has received the most attention is self-assembling multilayers (SAMs), with a focus on the layer-by-layer (LBL) approach [91-93, 95]. For this technique, oppositely charged polyelectrolyte layers are brought together by electrostatic forces which provides great stability and ease of synthesis.

Of the coating materials described earlier, PPy has been explored extensively for SAMs, due to its net positive charge [96-103]. In one of the earliest applications of such systems, a negatively charged layer of sulfonated polystyrene (SPS) was polymerized and later dipped into a solution of positive PPy [97]. This process allowed for attractive forces between the SPS and PPy layers, creating a very stable coating with thickness of only 150 angstroms [97]. This assembly was further enhanced with the addition of insulating layers, made with poly(thiophene-3-acetic acid)/polyallylamine (PTAA/PAH) produced with a

similar technique, where each block possessed a thickness of about 20 Angstroms [104]. Utilizing these charge-based self-assembly technique it is possible to obtain designs that, when used in biosensors, can offer a combination of the desired properties of low interference (from insulating polymers) and high conductivity (from conductive polymers).

Incorporating nanostructures like gold nanoparticles and carbon nanotubes into SAMs, very complex architectures can be generated [102, 105-113]. Shown in Figure 6 is an example of such intricate assembly, generated with the purpose of analyzing glucose levels [114]. It consists of an gold (Au) electrode, painted with an indium tin oxide (ITO) layer, onto which a layer of polyvinyl siloxane (PVS) layer is placed, followed by a self-assembling layer of poly(amido amine) (PAMAM) dendrimers. Upon three layers of these coating, a layer of cobalt hexacyanoferrate is added as the last step. Glucose Oxidase (GOx) is then immobilized on the surface along with a supportive protein of Bovine Serum Albumin (BSA) to achieve a final design of Au-ITO-(PVS/PAMAM-Au)<sub>3</sub>@CoHCF-GOx [114]. This design shown great parameters of conductivity and sensitivity, while the self-assembling aspect of the coating allowed for relatively easy manufacturing [114].

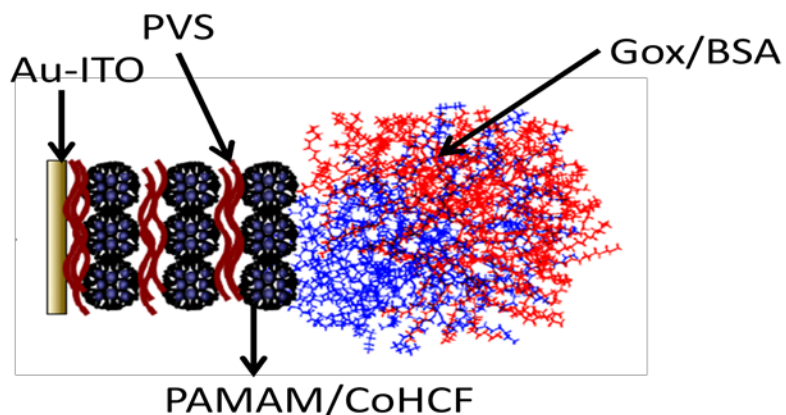


**Figure 9: Example of a complex architecture that can be obtain by the SAM technique.**  
Image source [116]

Aside from multiple layers, nanomaterials can also be simply dispersed inside a layer of polymer which have also demonstrated high sensing capabilities [115-119]. Multiple material can be brought together into a coating on a macroscale as well, while still maintaining stability and low thickness. One such technique was described by Barton et al [120]. An insulating layer of polydiaminobenzene (PDB) was first assembled onto a carbon electrode with a thickness of about 100nm [120]. This layer was then ablated with, in order to form pores. Subsequently, a conductive polymer (polyaniline) was used to fill out the pores, which resulted in a design resembling a protruding mushroom, as shown in Figure 7.

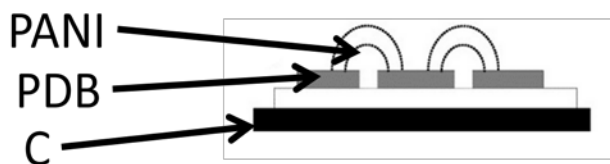


**Figure 10: The mushroom assembly.**

As can be seen from this review, the current state of research is focused on enhancing sensing capabilities while the expansion of biosensor technology to new applications remains very limited. This project focuses on expanding the use of electrochemical biosensors for monitoring of GBM.

#### **2.3.4.4 Enzyme-immobilization Technologies**

There are four methods of immobilizing proteins: adsorption, entrapment, covalent coupling and crosslinking. Adsorption is a physical, reversible process that is cheap and simple to perform while maintaining the activity of the enzyme [121-124]. The matrix and protein are joined by ionic or hydrophobic bonds. There is low stability however, and the enzyme may dissociate with changes in temperature, pH or surrounding solvent[123]. Due to the ease of synthesis associated with this method, considerable research has been

performed to optimize it. One of the most common techniques of performing the adsorption is with the use of the Langmuir-Blodgett method. The Langmuir-Blodgett was described earlier for the assembly of monomolecular multilayers, but it can also be utilized for the immobilization of enzymes [93, 94]. This technique is quick and easy to use and gives high control over the architecture of the coating, with adsorption depth as low as 1nm[102]. Another physical immobilization method is entrapment, where the enzyme is inserted within the pores of a crosslinked network, without forming any bonds with the surroundings. This method is yet again susceptible to temperature and pH denaturation [121].

With the covalent-binding method, covalent bonds are formed between inactive functional groups of enzyme and functional groups of the coating matrix, resulting in a very stable immobilization [121, 125, 126]. Enzyme groups that form covalent bonds are usually amino, carboxyl and hydroxyl groups [126]. Unlike the previous method, the immobilization process is performed in three distinct steps: (1) activation of carrier; (2) coupling of enzyme within a support material such as Sepharose, cellulose or silicates; and (3) removal of enzyme from the support material [126]. While this process is more complicated, covalent bonds will allow the enzyme to withstand most temperature and pH changes as well as remain stable over time [121, 126, 127].

For the method of crosslinking, an outside crosslinking agent is used to bind the enzyme to the coating material. The crosslinking agent, such as cyanogen bromide, carbodiimide, glutaraldehyde, aminosilane, diazonium salts, acid chloride, or isocyanate, is chosen to not match the functional groups that are present in the enzyme's active site [121, 127]. In the rare case that a crosslinking agent that needs to be used binds to the active site,

a competitive inhibitor may be used to take the place of the substrate on the enzyme while the crosslinking is taking place, which is then removed once the immobilization is achieved.

All four immobilization techniques have been utilized in the field of biosensor, however, when the desired effect is to maximize the stability of the system, a chemical immobilization method is preferred. On the other hand, when ease of synthesis is a major concern, a physical immobilization approach is used, such as the Langmuir-Blodgett[121]. A more innovative technique that was recently introduced in the field of biosensors is the elimination of the enzyme all together, to perform the biorecognition function with the use of a molecularly imprinted polymer (MIP) [128-133]. MIPs are smart, artificial systems that mimic the behavior of enzymes or antibodies [53]. If they are mixed with the polymer, they can create a molecular template with pockets that can entrap a specific analyte. Chen et al. developed an amine-imide polymer with pockets that allowed for formation of hydrogen bonds with uric acid [131]. The level of uric acid was detected based on the formation of pores in the polymer as the uric acid functional groups bound to the pockets [131]. Because this concept was only introduced recently research must be done to optimize the selectivity and sensitivity of the systems first before being utilized for specific applications.



# Chapter 3

## Design Process

## 3.1 Project Basics

The initial aspects of the project are considered below.

### 3.1.1 Project Stakeholders

The main stakeholders of this project are identified as follows:

- **Designers:** Thomas Jones, Nesa-Maria Anglin, Ana Dede, Courtney Rosales
- **Client:** Anjana Jain, Ph.D., Susan Zhou, Ph.D.
- **User:** Any medical staff treating glioblastoma multiforme

This is a first generation Major Qualifying Project, and any design or research presented herein is not a continuation of past projects.

### 3.1.2 Initial Statement

The following is the initial statement received from the client prior to the beginning of the project and provides a starting point to identify the goals of the team:

**Design an enzymatic coating for a biosensor to detect metabolite levels in cancer.**

### 3.1.3 Revised Client Statement

After conducting extensive background research consisting of literature reviews as well as client interviews in order to identify the design criteria, the team has revised the initial client statement to read as follows:

**Design a multi-metabolite biosensor using direct electron transfer (DET) to detect lactate and glutamate levels in glioblastoma multiforme (GBM), based on a 3mm carbon electrode provided by the client. The electrode coating must support immobilized lactate oxidase and glutamate oxidase that will be selective for the two metabolites. It should be stable for at least 21 days and sensitive to the nano-Molar level. The biosensor will deliver quantitative, real time data with an effective response time. The data generated by one device as well as data generated across device batches should be 95% reproducible. The electrical signal will be processed**

**using an Autolab processing unit which will then display a quantitative comparison between GBM and healthy tissue based on a standard curve developed by the team. The focus of this project will be to generate an in vitro proof of concept of the design.**

Justifications for changes made in the revised client statement are outlined below:

- **GBM** was chosen due to its aggressiveness, high rate of recurrence, and its distinct metabolic changes.
- A **multi-metabolite** biosensor will allow for a more precise monitoring of GBM.
- **Lactate** was chosen as a metabolite due to its significant concentration changes in all malignant cancers. **Glutamate** was chosen due to its specificity to astrocytoma.
- **Lactate oxidase** and **glutamate oxidase** were chosen based on their biological selectivity of the chosen metabolites.
- The biosensor should be **stable for 21 days** since this is what has been optimized by current methods [134-136].
- The **sensitivity must be at the  $\mu\text{M}$**  level in order to detect changes in glutamate concentration which is the limiting factor.
- The team wants the produced data by the design to be **reproducible 95% of the time** to provide confidence in measuring ability.
- The team will focus on ***in vitro* proof of concept** since this is a first generation project.

### 3.2 Objectives

The objectives for this project were generated from the client statement and the scope of the Worcester Polytechnic Institute Major Qualifying Project. From these criteria an objectives tree was drafted to outline the goals of the design as can be seen below in Appendix 3.

### 3.2.1 Primary Objectives

The primary objectives for this design were taken from the first level of branches in the objectives tree pictured in Appendix 3A. A pairwise comparison chart created to prioritize the primary design objectives can be seen in Appendix 3B. The team ranked monitoring ability as the highest priority, followed by adaptability, ease of use, and cost effectiveness.

**Monitoring ability** – The device must be able to monitor and accurately measure concentration levels of metabolites.

**Ease of use** – The device should be relatively easy to operate for the user and data presented should be easily interpreted.

**Adaptability** – The system should be designed to be easily adaptable to measure multiple metabolites simultaneously.

**Cost Effective** – The device should be able to be produced at the lowest possible cost.

### 3.2.2 Secondary Objectives

A set of secondary objectives, generated to help achieve the primary objectives, is shown in the second level of branches in the objectives tree in Appendix 1.

#### **Monitoring Ability:**

**Sensitivity** – The device should be sensitive to the microMolar ( $\mu\text{M}$ ) scale when measuring metabolite concentrations in healthy and malignant cells.

**Selectivity** – During the monitoring process, the enzymes should specifically target and interact with only the metabolites of interest.

**Response time** – The device should deliver measurements and quantitative data in as close to real time as possible.

**Stability** – The device should maintain monitoring ability and effectiveness over a prolonged period of time under physiological conditions

In Appendix 3B is a pairwise comparison chart created to prioritize the secondary design objectives specific to monitoring ability as displayed. The team ranked sensitivity and selectivity as the highest priority, followed by reproducibility, stability, and response time.

#### **Manufacturability:**

**Reproducibility** – The device should provide measurements that can be reproduced not only in one electrode but also across batches of electrodes.

**Ease of Production** – The device must be relatively easy to produce.

#### **Interference:**

**Isolating from Environment** – The device must be isolated from the environment in order to decrease interference from other electroactive or potentially degradative biological agents.

**Isolating reaction products** – The device must be able to isolate the generated products from the catalyzed reactions.

### **3.3 Constraints**

In the design of this project the team was constrained by the following criteria:

**Budget** – The design team was constrained to a budget of \$508.

**Time** – The project must be completed by the end of the 2013 academic school year.

**Sensitivity level** – In order to obtain quantitative data, the device must be sensitive to the  $\mu\text{Molar}$  level when measuring metabolite concentrations.

**Compatibility with provided electrode** – The design must be integrated and compatible with the 3mm carbon electrode provided by the client.

***In vitro* proof of concept** – As a bare minimum an *in vitro* proof of concept must be established.

**Processing Unit-** The design team was constrained to the provided software, Autolab PGSTA12 electrochemical workstation to collect data in lab.

### 3.4 Project Approach

The underlying goal of the project was to establish *in vitro* proof of concept that biosensor technology can be applied to GBM, by utilizing the mechanism of metabolite concentration changes. The project was broken down into six stages: research, design, prototyping, testing, design reiteration and documentation.

#### 3.4.1 Research

In order to get an understanding of the scope of the project, research was conducted on two main fields: GBM and biosensors. Research in the field of GBM was focused on the following topics:

- Existing monitoring strategies and need
- Biology and chemistry of GBM, with a particular consideration for changes in metabolic pathways
- Specific levels of metabolite concentrations for healthy and GBM tumor tissue, to use as a reference point.

Research in the field of biosensors was focused on the three main parts of a biosensor system: biorecognition, transduction, and processing. This research was divided among all four members of the group and it was assigned according to prior expertise of members in specific fields. Information was gathered from textbooks, peer-reviewed journal articles, patents, and interviews.

#### 3.4.2 Design

The designing stage of this project was broken down into two subparts:

### **a. Identifying Design Criteria**

Based on the knowledge gained from the literature review as well as from client interviews, the initial client statement was revised to contain feasible design objectives, constraints, and specifications for the functions of the device. The processing part of the device was specified according to the electrode-receiver system provided by the client, and prior experience of the group members with data processing software. From this point on, the design was focused only on the biorecognition and transduction aspects of the biosensor.

### **b. Generating Design Alternatives and Selecting a Design**

Based on the parameters identified above, the design criteria were narrowed down further to enzyme immobilization and coating technology for the enhancement of both biorecognition and transduction for a GBM biosensor. Several approaches were utilized in order to generate design alternatives. A more thorough literature and patent search was first performed in these particular areas, followed by brainstorming and iterative sketches within the group, in order to compile seven design alternatives.

A quantitative and qualitative metrics system was used to rate the different design alternatives against the constraints and objectives. The highest scoring alternative was selected as the winning design.

### **3.4.3 Prototyping**

A detailed protocol was first put together for the prototyping of the design including three major components:

1. Method for synthesis of coating
2. Method for immobilization of enzyme

### 3. Method for linking the coating to the provided electrode.

The team followed the specified protocols closely to build the prototype.

#### 3.4.4 Testing

Once the design was manufactured, a variety of experiments were conducted to establish proof of concept. One set of experiments was done to analyze the parameters of the design. The first experiment consisted of examining the conductivity of the coating. For this, current was passed through the coating in order to determine the quality of the signal, quantified as signal-to-noise ratio, as well as to determine the efficiency of conduction. The conductivity test was done on the coating alone, as well as on an enzyme-immobilized coating, to determine whether or not the enzyme interfered with the conductivity. Selectivity testing was performed next, to study the effect of the presence of potentially interfering agents. Sensitivity testing was then performed to determine the lowest concentration of metabolites that could be detected with the system, in order to verify that these levels are relatable to physiological levels.

Once the conductivity, selectivity and sensitivity were established, the next set of experiments focused on using the system for *in vitro* testing. The first experiment for this set consisted of establishing a standard curve for the metabolite readings to determine the relationship between the concentration of the metabolites and the voltage output. Once this relationship was determined, the biosensor could then be utilized for measurement of metabolite concentrations on *in vitro* cell cultures. Metabolite levels on two different cell lines were measured: in a GBM cell line and in a healthy astrocyte culture. The outputs were compared in order to established proof of concept that this method can be used to



distinguish between cancerous and healthy tissue. Next, the stability of the system over time was studied with the *in vitro* cultures, by examining the selectivity, sensitivity and conductivity of the measurements over time. The next experiments focused on reproducibility. Two aspects of the reproducibility of the data were studied:

- Reproducibility of data collected by one device
- Reproducibility of data collected from different device batches

Next, a double blind study was performed to detect the presence or absence of GBM on a cell culture of unknown origin, to determine the accuracy of the standard curve conversions. As a concluding step, the biosensor that was developed was used for an *in vitro* treatment monitoring study. A therapeutic agent of established efficacy was administered to a GBM cell line to simulate the treatment of a patient. The biosensor was used to collect data at different time points during the treatment, to measure the metabolite concentration changes over time. Based on the fact that this agent is known to negate GBM, the response that is received by the biosensor will provide *in vitro* proof of concept, which is the ultimate goal of the project.

#### **3.4.5 Design Reiteration and Documentation**

Based on the results from the aforementioned experiments, the biosensor design was modified to improve its capabilities and behavior. A cycle design approach was utilized, where after each iteration of the system new tests were run to ensure best possible refining for the design. Project progress was documented every day in the lab notebook, summarized in weekly progress reports and organized in chapter format at the end of each term. A final project report was then assembled at the end of the project.

# **Chapter 4**

## **Design Process**

#### 4.1 Need Analysis

Glioblastoma affects 17,000 people every single year and has a two-year survival rate of only 3%, even with cutting edge treatment. The high recurrence rate and aggressiveness of glioblastoma creates a need for proper monitoring of the disease after treatment to determine its efficacy. Magnetic Resonance Imaging (MRI) and Computed Tomography (CT scan) are the most common monitoring methods for GBM. While both methods show a great leap in the evolution of technology, they both present certain limitations. The low contrast resolution of an MRI makes it difficult to distinguish between healthy brain tissue and diseased tissue until the cancer progresses to a certain size. CT scans are harmful to the patient's healthy cells as the radiation can damage DNA.

Due to their ability to convert a biological response to an electrical signal, biosensors present a novel way to monitor the progression of GBM. The biosensor the team is designing will build upon current concepts in biosensor technology and will attempt to widen the applications of biosensors. This device will achieve an *in vitro* proof of concept, work along with an existing carbon electrode and Autolab PGSTA12 processing unit. The system will display the pathological state of GBM during treatment.

Our design will be effective as it meets and optimizes the needs of the client, which are:

- **Ability to distinguish between GBM and healthy brain tissue:** By using the metabolite levels present in the tissue and comparing them to the concentration standard curve, the team can determine whether or not the tissue is cancerous.
- **Sensitivity:** The device must be sensitive to the micromolar level in order to accurately detect concentration changes.
- **Stability:** The device must be stable enough to monitor GBM throughout a normal treatment regimen.

- **Compatibility with existing electrode:** The design must be compatible with a 3mm carbon electrode.
- **Biocompatibility:** The materials used must not cause or induce a foreign body response for future *in vivo* applications.

Our client has highlighted some features that they would like to be incorporated into the overall design of the project, however, due to the timeline of the project and the budget, the team will prioritize the focus of this project on the needs, while attempting to address all the features the client wants, which are as follows:

- **Adaptable to smaller electrode arrays:** The device should be optimized for use with any size electrode.
- **Implantable:** The biosensor should be designed to be utilized *in vivo* while staying minimally invasive and inducing minimal scar tissue formation.
- **Able to monitor multiple metabolites:** The system should effectively monitor the levels of multiple metabolites simultaneously without causing interference.
- **Quick response time:** The device should be able to display the concentration of metabolites as close to real time as possible.

Based on the wants and needs of the client, the functions and specifications of the design can be determined.

## 4.2 Functions

The overall function of the device is to detect metabolite changes in GBM in order to gain an understanding of its pathological state. However, there are discrete sub-functions that must be performed to achieve the main function. A black box diagram was used as a tool to generate these sub-functions. The initial input into the system is the metabolite of interest that is being measured. The final output is the pathological state of the GBM tissue that is being monitored. Specific functions were established within the black box to

determine how the initial input is converted into the final output. The black box diagram that was developed can be seen below in Figure 8.

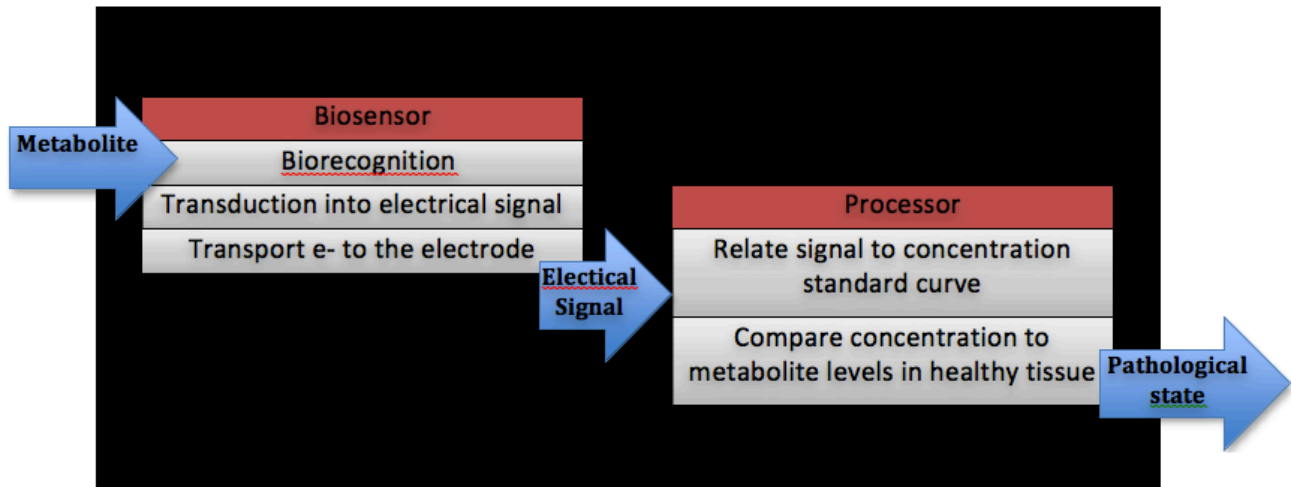


Figure 11: A black-box diagram showing the functions of the device.

As can be seen in Figure 8 the black-box diagram is split into two sub-systems, the biosensor unit and the processing unit. The output of the first system is the input for the second.

- **Biorecognition:** The device must be able to selectively recognize the metabolite that is being targeted for measurement without interacting with any other substrates.
- **Transduction:** The device must be able to convert a biological signal into an electrical signal in order to provide quantitative data.
- **Conduction:** The signal must be isolated and collected at the electrode, so the device must be able to conduct the generated electrical signal from the biorecognition agent to the electrode. At this point the signal will be picked up and transported to the processing unit.
- **Process signal:** The quantity of electrons will be compared to a predetermined concentration standard curve which provides a function that describes the direct

relationship between the number of electrons and the concentration of that metabolite. The processing unit must be able to compare these concentrations to levels measured in healthy tissue and provide the pathological state of the GBM tissue.

### **4.3 Specifications**

In order to achieve these functions, the device must comply with the specifications determined through client interviews and extensive literature review.

#### **4.3.1 Metabolites**

The team decided on measuring the metabolites lactate and glutamate based on findings in the literature. The metabolisms of all types of tumor tissues produce an elevated concentration of lactate. These levels can be measured and then compared to healthy lactate levels to determine a pathological state. Additionally, astrocytic tumor cells are known to produce elevated levels of glutamate. Therefore, lactate and glutamate will be chosen as the specific metabolites targeted by the biosensor.

#### **4.3.2 Biorecognition and transduction agent**

Enzymes were initially suggested by the client as the biorecognition agent, which the team supported due to the fact that enzymes serve the dual purpose of both biorecognition as well as transduction into an electrical signal. Enzymes are biological molecules that specifically bind to a specific substrate and catalyze chemical reactions. Enzymes are divided into a number of different classes that yield different products. For instance, a dehydrogenase is an enzyme that activates oxidation-reduction reactions by transferring hydrogen from substrate to acceptor. Because the biosensor needs to measure an electrical signal in order to determine the pathological state, an enzyme that produces a high concentration of electrons as a byproduct of the reaction is necessary. Therefore the oxidases were the best choice, producing hydrogen peroxide which can then be further

reduced to electrons. For these reasons, lactate oxidase (LOx) and glutamate oxidase (GLOx) were chosen to specifically bind with the metabolites.

### 4.3.3 Sensitivity and Range

In order to determine the pathological state from the measured level of metabolites it is necessary to establish what metabolite concentrations constitute healthy and malignant tissue. The concentrations were from a study performed in rats and can be seen in Table 3 [137].

**Table 3: Systemic concentration levels of metabolites in healthy vs. malignant tissue of rats [25].**

Metabolite	GBM ( $\mu\text{M}$ )	Healthy ( $\mu\text{M}$ )
Lactate	424.1 $\pm$ 185.9	248.9 $\pm$ 110.3
Glutamate	5.06 $\pm$ 3.88	1.3 $\pm$ 0.32

### 4.3.4 Dimensions

The dimensions of the biosensor are specified by the electrode provided by the client. The electrode is carbon based and 3mm in diameter. Therefore, the design of this biosensor is limited to a 3mm diameter.

### 4.3.5 Stability

The biosensor must be stable for a period of time that allows for the monitoring of GBM progression. Based on the current state of biosensors in the literature, a stability timeframe of at least 21 days was established.

## 4.4 Design Alternatives

Before generating design alternatives, the team created a morphological chart to develop different means for performing each of the desired functions. The morphological chart is based on function analysis, where each of the functions is listed on the left column while the different methods or mechanisms which can be used to perform the functions are listed in the rows. The morphological chart can be seen in Appendix 4A

#### **4.4.1 Developing Design Alternatives**

Each of the team members utilized the morphological chart during an individual brainstorming period to generate sketches of possible design alternatives. The ideas were presented and reiterated through discussions and an additional brainstorming session. From this, the team was left with twelve final design alternatives. During the design process, the team decided to focus on the mechanism and not the specific materials involved ensuring that the designs were not being limited by specific material choices. Instead the type of material was the focus, whether it was conductive, nonconductive or a type of nanostructure. The team would later rank the specific materials and insert them into the final design.

#### **4.4.2 Design Alternatives**

The design alternatives generated by the team are coatings for the provided electrode. The designs fall into two main categories – those that contain two enzymes and those that contain only one enzyme. The design alternatives that contain only one enzyme contain the selective oxidase enzyme that breaks down the metabolite of choice into products that include hydrogen peroxide. The design alternatives that contain two enzymes also incorporate horseradish peroxidase (HRP). This enzyme targets hydrogen peroxide and catalyzes the breakdown of it into free electrons. The reason for including the HRP is to mitigate the problem of the hydrogen peroxide being unable to diffuse through the polymer to the electrode that is encountered in some biosensor designs. The only drawback to the use of two enzymes, however, is the increase cost associated with using both.

There are two classes of coatings used in different ways in the design alternatives, non-conductive and conductive coatings. The purpose of non-conductive coatings in



designs is to decrease the interference with electroactive particles that can be found in a biological environment and also to help isolate electrons within the biosensor system. Conductive coatings are used with the goal of increasing the conduction of free electrons generated from hydrogen peroxide breakdown to the electrode.

The following symbols were used for the design sketches:

 or  - Horseradish Peroxidase (HRP)

 or  - Lactate Oxidase (LOx)

### 1: Mushroom

The first design alternative mimics the shape of a mushroom. This coating consists of a non-conductive polymer layer with pockets of a conductive polymer throughout the entire layer. Each of the pockets has a hemispherical drop of conductive polymer on the top of the pocket. The conductive polymer contains both the oxidase enzyme and HRP dispersed throughout. The hemispherical design serves to increase the surface area where the metabolite of choice can interact with the selective oxidase enzyme. This design can be seen in Figure 9.

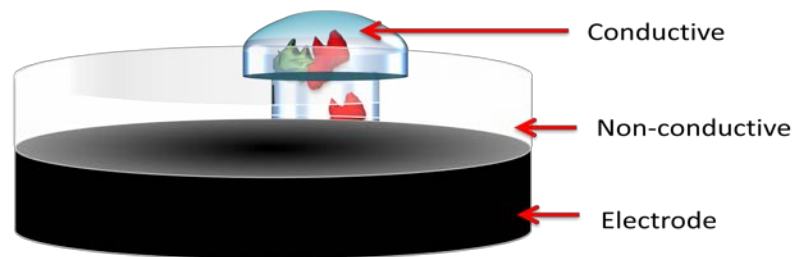


**Figure 12: Mushroom design.**

## **2: CNT Towers**

This design alternative uses two different materials, a conductive polymer and carbon nanotubes (CNT). In order to manufacture this design, the carbon nanotubes would be deposited onto the electrode and aligned perpendicular to it. The carbon nanotubes would contain HRP attached to their surface. Then, areas of the CNTs would be removed and a conductive polymer with both enzymes contained in it would be polymerized in the removed areas. This design would allow the metabolite of choice to react with the oxidase enzyme in the conductive polymer. Then the resulting hydrogen peroxide would interact with the HRP in the polymer, and any hydrogen peroxide that began to leave the area of the biosensor would react with the HRP on the CNTs. The CNTs would conduct the free electrons created back to the electrode. This distinguishing feature of this design is to increase the sensitivity by decreasing the amount of hydrogen peroxide that is able to escape the biosensor construct. This design can be seen in Figure 10.

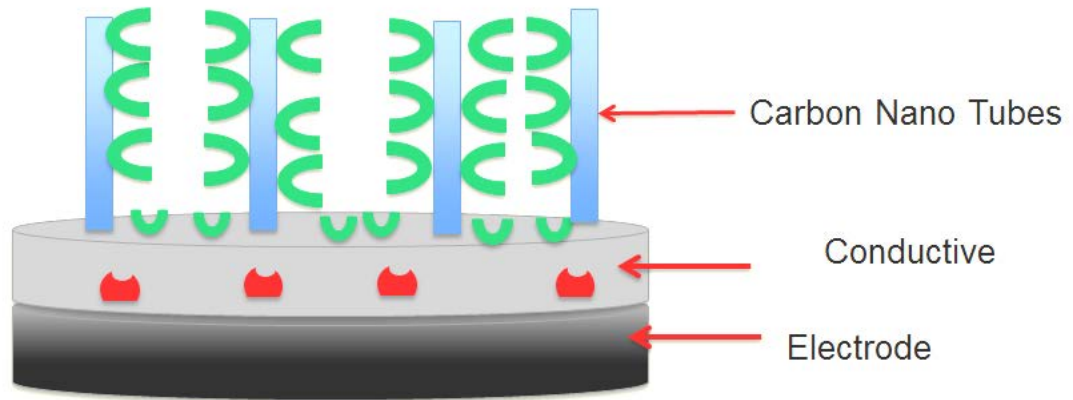


**Figure 13: CNT Towers design.**

### 3: CNT Bed

The CNT bed design alternative consists of a layer of non-conductive polymer that contains CNTs. This mixture would be deposited onto the electrode, and both types of enzymes would be attached to the surface of the composite. The CNTs would be aligned perpendicular to the electrode and serve to conduct the generated free electrons to the electrode. Since they are contained in a non-conductive polymer, the CNTs would be isolated from any interference from other electroactive agents that can be present in a physiological environment. This design can be seen in Figure 11..

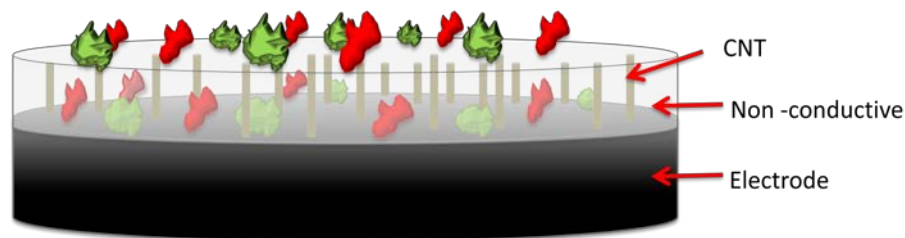


**Figure 14: CNT Bed design.**

### 4: Smart Polymer

This design alternative incorporates the use of a smart polymer that is sensitive to pH changes in its environment. The smart polymer contains both the oxidase and HRP enzymes throughout it. A non-conductive membrane is placed over the smart polymer. At

normal pH, the smart polymer exists in a solid state. However, as the hydrogen peroxide is broken down, H<sup>+</sup> ions are generated which would decrease the local pH around the smart polymer. Once the pH is lowered enough, then the smart polymer would transform into a hydrogel, which would allow the hydrogen peroxide to easily diffuse into it. This design can be seen in Figure 12.

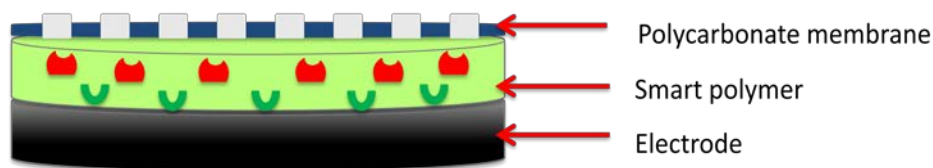


**Figure 15: Smart Polymer design.**

### 5: Single Layer

This design is one of the simpler design alternatives. It consists of only one a layer of conductive polymer that contains both enzymes throughout it. The advantage of this design is its simplicity, as it can be developed easily and consistently. This design can be seen in Figure 13.

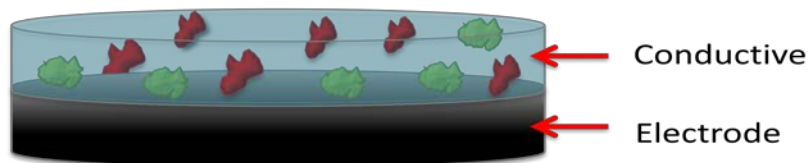


**Figure 16: Single Layer design.**

### 6: Bilayer

This design alternative is very similar to the single layer design, but adds a second layer to it. The first layer consists of a conductive polymer with the HRP and oxidase enzyme throughout it. The second layer is a porous non-conductive polymer. The reason for the addition of a second layer is to decrease interference as well as to better contain the

hydrogen peroxide generated by the breakdown of the metabolite of choice. This design can be seen in Figure 14.

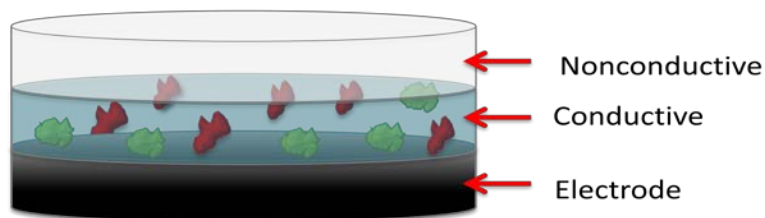


**Figure 17: Bilayer design.**

### **7: Tri-layer**

The Tri-layer design alternative consists of three different layers. The first layer is a conductive polymer that is deposited onto the electrode. Both of the enzymes that are used are contained in this layer. The second layer is a non-conductive polymer that contains only the HRP enzyme in it. The third layer is only a non-conductive polymer. The second layer serves to trap any hydrogen peroxide that may escape the area of the biosensor by the HRP catalyzing its breakdown into free electrons. The third layer is added in order to diminish the ability of any hydrogen peroxide in the environment to interact with the HRP in the second layer. This design can be seen in Figure 15.

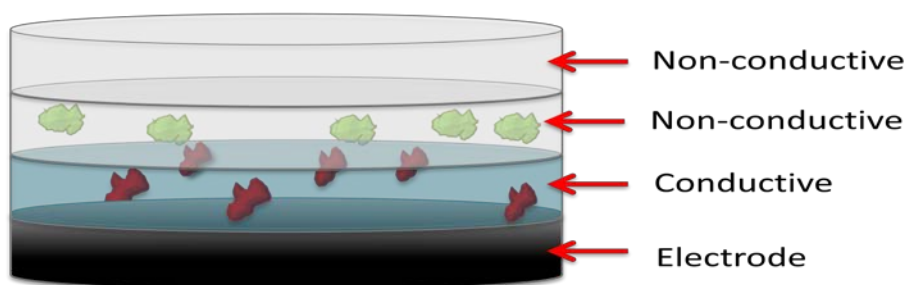


**Figure 18: Tri-layer design.**

### **8: Single Layer with Surface Indentations**

This design alternative is similar in function to the single layer design. This design, however, consists of indentations made on the surface of the conductive layer. The added

indentations serve to increase the surface area of the coating, thereby increasing the ability for the metabolite to interact with the oxidase enzyme. This design can be seen in Figure 16.



**Figure 19: Single Layer with Surface Indentations.**

### 9: Nanovelcro

This design consists of two separate components. A conductive polymer layer that contains HRP and the oxidase enzyme is polymerized on the surface of the electrode. Then, a polymer membrane that is manufactured to have nanovelcro hooks on a single side is placed over the conductive layer with the hooks facing the electrode. These nanohooks would create one way channels through which metabolites could enter the biosensor system since they would block and prevent molecules from exiting the pores of the membrane. This design can be seen in Figure 17.

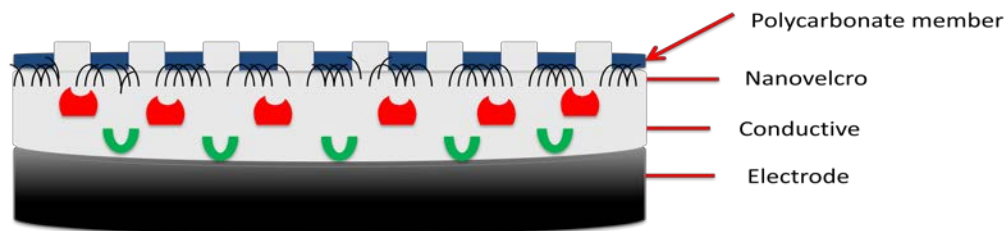


**Figure 20: Nanovelcro design.**

### 10: One Enzyme Mushroom

This design alternative is the same as the mushroom design, however it does not utilize the HRP enzyme. The conductive polymer used in this design only contains the

metabolite selective oxidase enzyme. Otherwise, it operates and would be developed the same way as the mushroom design. This design can be seen in Figure 18.

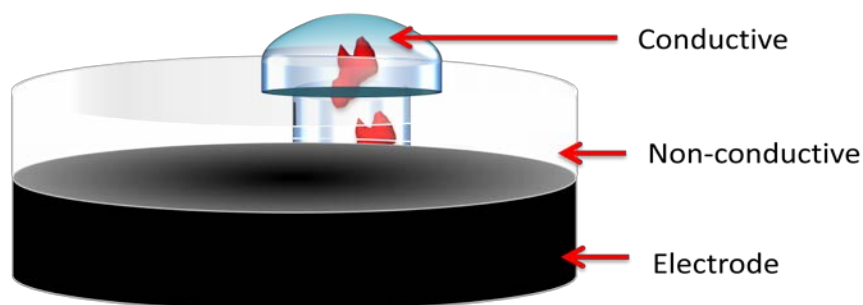


**Figure 21: One Enzyme Mushroom design.**

### **11: One Enzyme Single Layer**

This design is similar to the single layer design, however it does not contain the HRP enzyme. It is the simplest of all the design alternatives, and consists solely of one layer of conductive polymer with an oxidase enzyme throughout it that is deposited onto the surface of the electrode. This design can be seen in Figure 19.

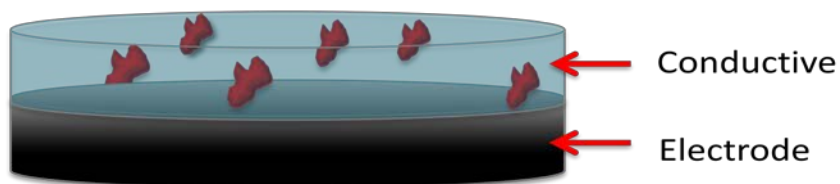


**Figure 22: One Enzyme Single Layer design.**

### **12: One Enzyme Bilayer**

This design alternative uses only the oxidase enzyme and no HRP. The way in which it is created and works is identical to the bilayer design alternative. A conductive polymer layer containing only the oxidase enzyme is polymerized on the surface of the electrode,

and a non-conductive polymer layer is placed on top of it. This design can be seen in Figure 20.

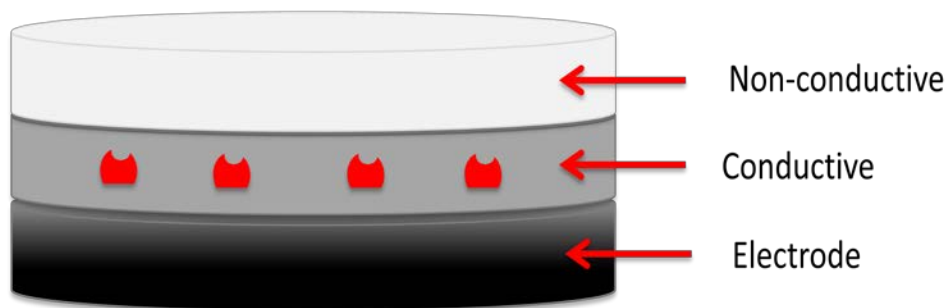


**Figure 23: One enzyme bilayer design.**

#### **4.5 Design Alternative Evaluation**

After generating the 12 design alternatives the team developed criteria in order to evaluate each of the designs.

##### **4.5.1 Evaluation of Materials**

The 12 design alternatives were generated based on general classes of materials: conductive and non-conductive. Before ranking the designs against each other the team produced potential lists for materials that fall under these classes and ranked them based on biocompatibility, cost, ease of synthesis and processability, conductivity, enzyme immobilization, and stability of each material. The final material choices were applied to all 12 designs and the final scores for each of the materials along with explanations can be found in Appendix 3B.

##### **4.5.2 Evaluation of Design Alternatives**

After the generation of twelve design alternatives, the team ranked each one to decide on the final design. The evaluation of the design alternatives was performed as objectively as possible, with quantification of design objectives wherever possible. The



four top level objectives of the device were assigned numerical values, weighted based on the pairwise comparison chart that can be seen in Appendix 3B. This led to the following score breakdown, with the maximum possible score being a 100:

- Monitoring Ability: 40 Points
- Manufacturability: 30 Points
- Interference: 20 Points
- Cost: 10 Points.

#### **4.5.2.1 Monitoring Ability**

The monitoring ability objective was broken down into sub-objectives and assigned weights based on the pairwise comparison chart of secondary objectives seen in Appendix . This led to the following score breakdown:

- Sensitivity: 13 points
- Selectivity: 13 points
- Precision: 6 points
- Stability: 6 points
- Response time: 2 points

Each of the design alternatives were assigned scores for each of the sub-objectives.

Final results and explanations for scoring can be found in Appendix 4B.

#### **4.5.2.2 Manufacturability**

Manufacturability was broken down into two sub-objectives:

- Ease of production: 25 points
- Reproducibility: 5 points

The point values of the objectives were agreed upon by team consensus, with the thought that ease of production was of paramount importance due to the time constraints on the project. While reproducibility, meaning how easily the manufacturing protocol can

be exactly replicated, is important, the team decided to focus on an easy to produce design. The final scores attributed to each design alternative, along with explanations can be found in Appendix 4C.

#### **4.5.2.3 Interference Reduction**

The objective of interference reduction was broken down into two sub-objectives that were determined to be of equal importance:

- Isolation from environment: 10 points
- Isolating electrons in device: 10 points

Isolation from environment entails blocking the sensing system from electroactive particles that may be present in a biological setting that could cause interference with the accuracy of the measurements. Isolating electrons in the device is the goal of not allowing free electrons generated by the breakdown of  $H_2O_2$  to exit into the aqueous environment without being conducted into the electrode. By achieving this objective, the sensitivity of the device can be optimized. The final scores for each of the design alternatives along with explanations can be found in Appendix 4D.

#### **4.5.2.4 Cost**

The final objective that the design alternatives were total cost, determined based on the individual materials as shown in Appendix 4D.

#### **4.5.3 Final Design Alternative Scores**

After evaluating each of the twelve design alternatives for each of the four main objectives of the device, these values were summed to generate the final score for each design. These outcomes can be seen in Table 4 below.

**Table 4: Evaluation of the 12 designs based on the project objectives.**

	1	2	3	4	5	6	7	8	9	10	11	12
Monitoring Ability	32	40	36	33	32	34	31	30	34	28	28	30
Manufacturability	24	10	13	17	29	18	12	21	8	24	29	18
Interference	10	10	5	15	0	15	20	0	20	10	0	15
Cost	7.5	2.5	2.5	5	7.5	7.5	7.5	7.5	5	9	10	9
<b>Total:</b>	<b>73.5</b>	<b>62.5</b>	<b>56.5</b>	<b>70</b>	<b>68.5</b>	<b>74.5</b>	<b>70.5</b>	<b>58.5</b>	<b>67</b>	<b>71</b>	<b>67</b>	<b>72</b>

The highest scoring design is the Bilayer followed by two other designs with equal scores: the Single Layer and the Mushroom, each with a total of 73.5.

#### **4.6 Final Design**

Among the 12 design alternatives, two designs were favored based on their high ranking in the evaluation matrix. However, choosing one of these alternatives over the other was a difficult task. An in-depth analysis of the factors influencing the performance of each design was necessary before a decision could be made on the optimal choice.

One approach that can be used for this analysis is a theoretical one, where laws of diffusion, mass transfer and chemical reaction rates are analyzed for each conceptual design. In particular, one would have to determine the level of diffusion of metabolites and of H<sub>2</sub>O<sub>2</sub> through the films which is controlled by several factors: the concentration of the compounds in the local area, diffusivity of the compound, permeability of the film, as well as thickness of film. The effect of the reaction surface area on the performance of the device is yet another parameter that needs to be analyzed in order to choose one design over the other. These parameters are described more in depth below:

- Diffusion of metabolites through Chi depends on the gel thickness, porosity and pore size, metabolite concentration, metabolite molecular weight, and interaction of metabolites with Chi.
- Diffusion of H<sub>2</sub>O<sub>2</sub> depends on the thickness, porosity and pore size of PPy, concentration of H<sub>2</sub>O<sub>2</sub> produced, H<sub>2</sub>O<sub>2</sub> molecular weight, as well as the interaction of H<sub>2</sub>O<sub>2</sub> with the PPy. Both designs operate on the principle of minimizing the need for diffusion of H<sub>2</sub>O<sub>2</sub> to the electrode by providing the HRP enzymes on the surface of the coating for immediate break down to free electrons. However, depending on the level of H<sub>2</sub>O<sub>2</sub> produced, this approach may not *fully eliminate* the need for some diffusion of H<sub>2</sub>O<sub>2</sub> through PPy to ensure full breakdown.
- Reaction rates depend on the concentration of substrates and enzymes, as well as the speed of freeing of enzymes after each reaction.

Based on these factors, the advantages and limitations of each design can be analyzed as follows:

- The bilayer design offers a larger surface area for the reaction to take place however it requires the diffusion of metabolite through Chi before the initiation of the reaction.
- On the other hand, the mushroom design eliminates the need for the diffusion of metabolites however offers a smaller surface area for the reaction to happen.

The theoretical approach to weighing the advantages and limitations in order to pick the best alternative proved to be challenging due to (1) the lack of existing literature utilizing these particular design geometries, (2) the complexity of the concepts involved, and (3) the significant number of assumptions that were necessary in order to perform the analysis, which limits the overall accuracy of the results. Instead of theoretical analysis, an experimental approach was determined to be more appropriate, where several device performance tests were conducted with *both* designs, and a final choice was made based on

the results. This approach was feasible due to the fact that the designs utilize the same materials, and therefore do not put a strain on the budget of this project.

Building both designs and choosing the best one was a multistage process, as summarized in Figure 21. It involved starting out with a simple idea and then slowly building up to more advanced concepts. Due to the complexity of the nature of this project, the slowly advancing approach was deemed to be more appropriate, compared to the technique of prototyping the final designs as conceptualized, running all tests and then reiterating the design. The step-by-step reiteration technique makes the process of troubleshooting the protocol more efficient.

The multistage process started out with a much simpler concept that could be traced back to the mechanism of both alternatives. As the first step, only one enzyme and only one coating were used: LOx was immobilized in PPy, while temporarily ignoring GLOx and HRP. LOx was chosen over GLOx for this step because there is more existing literature on the use of LOx for biosensors. Tests were run to determine the functionality of the design, and when negative results were obtained, the protocol of the process was iterated accordingly until the design functioned successfully.

The next step involved the immobilization of HRP in PPy, in addition to LOx. Once again, iterations were made to the protocols until successful results were obtained. The third step involved advancement in the protocol to utilize another coating: Chi. Two designs were built with the geometries of the two selected design alternatives: one with a Chi layer, encompassing the PPy layer all around, and one with a mushroom technique where the Chi layer was indented to include enzyme-immobilized PPy. Tests were run simultaneously and the design that performed best was selected as the final design. The

last step in the process was to utilize this final design to the construction of the same system for GLOx. The protocols were modified as needed according the test results.

The parameters of the designs were adopted from similar designs found in the literature, and by taking into consideration several hypotheses as summarized in Table 5. As can be seen in this table, obtaining the optimal design is a balancing act between maximizing the parameters to increase the positive effect, and minimizing the parameters to lower the negative effects. The parameters of the final design are summarized in Table 6. The diameter of the coating was determined by the diameter of the electrode as given by the client.

**Figure 24: Summary of the approach that was followed in this project in order to choose and optimize the design.**

**Table 5: Summary of hypothesis that were taken into consideration when determining the parameters for the final designs.**

Optimizing parameter	Positive effect	Negative effect
Maximizing the thickness of the PPy film.	Increases the amount of enzyme that can be entrapped in it, which improves the biosensor response.	Impedes complete diffusion of H <sub>2</sub> O <sub>2</sub> , which lowers the biosensor response.
Maximizing the thickness of the Chi film.	Decreases the interference, which improves the biosensor response.	Increases the distance the metabolites need to diffuse through which lowers the biosensor response.
Maximizing the surface area immobilized with enzymes.	Increases the rate of reaction which improves the biosensor response.	Increases the possibility of inference of other agents which lowers the biosensor response.

**Table 6: Summary of the parameters for the construction of the final designs. This chart is broken down based on the steps shown in Fig.21.**

Step 1		
Part	Parameter	Value
<b>Film</b>	Diameter of PPy coating	3mm
	Height of PPy layer	200µm
	Concentration of PPy	0.1M
	Volume of PPy	200m
	Concentration of Chi	N/A
	Volume of Chi	N/A
<b>Enzyme</b>	Concentration of LOx	100mg/mL
	Volume of LOx	10uL
	Concentration of GIOx	N/A
	Volume of GIOx	N/A
	Concentration of HRP	N/A
	Volume of HRP	N/A



Step 2		
Part	Parameter	Value
Film	Diameter of PPy coating	3mm
	Height of PPy layer	200 $\mu$ m
	Concentration of PPy	0.1M
	Volume of PPy	200m
	Concentration of Chi	N/A
	Volume of Chi	N/A
Enzymes	Concentration of LOx	100mg/mL
	Volume of LOx	10uL
	Concentration of GLOx	N/A
	Volume of GLOx	N/A
	Concentration of HRP	100mg/mL
	Volume of HRP	20uL
Step 3		
Part	Parameter	Value
Film	Diameter of PPy coating	3mm
	Height of PPy layer	200 $\mu$ m
	Concentration of PPy	0.1M
	Volume of PPy	200m
	Concentration of Chi	1M
	Volume of Chi	200 $\mu$ m
Enzyme	Concentration of LOx	100mg/mL
	Volume of LOx	10uL
	Concentration of GLOx	N/A
	Volume of GLOx	N/A
	Concentration of HRP	100mg/mL
	Volume of HRP	20uL
Step 4		
Part	Parameter	Value
Film	Diameter of PPy coating	3mm
	Height of PPy layer	200 $\mu$ m
	Concentration of PPy	0.1M
	Volume of PPy	200m
	Concentration of Chi	1M
	Volume of Chi	200 $\mu$ m
Enzyme	Concentration of LOx	N/A
	Volume of LOx	N/A
	Concentration of GLOx	100mg/mL
	Volume of GLOx	10uL
	Concentration of HRP	100mg/mL
	Volume of HRP	200 $\mu$ L

# **Chapter 5**

## **Methodology**

An overview of the methodology followed in this project is given below. For more details please reference Appendices 5A – 5G.

### 5.1 Film deposition

The purpose of depositing a PPy film is to facilitate the transfer of free electrons to the electrode and to immobilize the lactate oxidase.

A 3mm glassy carbon electrode (GCE) was polished in sequential steps of  $1\mu\text{m}$  and  $.3\mu\text{m}$  of alumina slurry followed by sonication in deionized water (DI) and ethanol for 5 min. Polypyrrole (PPy) (0.034 g), purchased from Sigma Aldrich (CAS# 30604-81-0), and  $30\mu\text{L}$  of lactate oxidase (LOx) (Sigma Aldrich, CAS# 9028-72-2) were added to 10mL of .1M KCl solution and degassed by nitrogen bubbling for 30 min. The PPy solution was then electrochemically deposited onto the GCE by passing a voltage of 0.75V between the GCE and an AgCl reference electrode (RE) for 1800s using the GPES software and AUTOLAB potentiostat (Metrohm). The electrochemical deposition setup is pictured below in Figure 22.



**Figure 25: PPy electrochemical film deposition set up**

## 5.2 Film characterization

Tests were performed after PPy film deposition on the electrode with and without LOx to characterize its properties and validate deposition.

### 5.2.1 Contact angle analysis

Contact angle analysis was used as a method to both quantify the presence of a PPy film on the GCE surface as well as to further characterize the film. The system used to perform the analysis consisted of a Shott power source, an Auto Dispensing system, a camera, a platform for the sample, and the DROP Image Standard software (Rame-Hart).

To test a GCE, the sample was first attached to the side of the platform using tape. The light source was turned to a power of 70 watts and placed on one side of the electrode. The camera was placed on the other side of the electrode. This setup results in a picture where the sample and water drop are black shadows against a white background. Prior to the picture being captured, it was ensured that the electrode was perpendicular to the plane of the camera. Once the DROP Image Standard software was loaded, the drop volume was set to 2 $\mu$ L. Then the Contact Angle tool was opened, a drop of DI water placed on the surface of the GCE, and an image taken of the sample. Two vertical lines were placed on the left and right sides of the drop applicator in the image by left and right clicking, respectively. A third horizontal line was placed flush with the surface of the sample, using the up and down arrow keys, and the Measure button was pressed in the software. The contact angles of the left and right sides of the drop, as well as the average of the two were then displayed.

### 5.2.2 Cyclic voltammetry

To confirm the presence of LOx immobilized in the film as well as prove that the PPy film does not add any impedance, cyclic voltammetry was performed on clean and modified GCE's in 100 $\mu$ M lactic acid. GPES software and the AUTOLAB system were used at a scan rate of 0.1V s<sup>-1</sup> between -0.6 and +0.2V. The results were then plotted on the same graph, and the difference between the oxidation points of a clean GCE and the modified GCE in 100 $\mu$ M lactic acid was calculated. This test was conducted 3 times for each condition.

### 5.3 Bench biosensor validation

A number of biosensor validation tests were performed using electrodes with deposited PPy films containing LOx and the AUTOLAB system. There were three main goals for this specific experiment. The first was to verify the presence of enzyme in the deposited PPy film. The second was to illustrate that the biosensor could respond to increasing lactate concentration by showing a system output change, thus validating the PPy with enzyme deposition protocol. Finally, a real-time lactate recognition test was conducted to verify that a real time response could be obtained with increasing lactate concentration.

#### 5.3.1 Lactate amperometry

To verify the PPy with enzyme deposition protocol and illustrate that the biosensor could respond to increasing lactate concentration by showing a system output change, lactate amperometry was conducted. This test was conducted by placing the GCE, RE, and WE in 10mL of the following lactate (Amresco, CAS# 50-21-5) concentrations: 1mM, 500 $\mu$ M, 100 $\mu$ M, and 500nM. A voltage of -0.2V was passed between the PPy modified GCE and the RE for 120s while the GCE was submerged in the lactate. This was repeated 3 times

with a different PPy modified GCE for each concentration and the results of each trial were then averaged. A standard curve was also generated based on the lactate concentrations used vs. the point on the graph at which the current leveled off. The setup of this experiment can be seen in Figure 26.



Figure 26: Set up of the lactate amperometry

### 5.3.2 Real time lactate recognition

To demonstrate that there is a system output increases with increasing lactate concentration a real-time lactate recognition experiment was conducted. A PPy modified GCE, RE, and WE were placed in a beaker containing 10mL of PBS. Ten 1mL drops of lactate concentrations ranging from 1nM-100M were added into the beaker every 60s. This was conducted three times with three different PPy modified GCE's and the results were averaged.

### 5.4 *In vitro* biosensor validation

The purpose of the *in vitro* biosensor validation tests were to obtain the concentration of lactate being secreted for various cell densities by using a commercial

colorimetric lactate assay and to determine the accuracy of the biosensor by testing in the same media and comparing to the results of the assay.

#### **5.4.1 Cell Culture**

U87mg glioblastoma cells were plated at nine different densities in regular media, with the total number of cells ranging from 25,000-1,500,000 cells. After 1.5 days the media was collected and the live cells were counted using Trypan blue. Then .5mL of collected media was then centrifuged using 7 kDA desalting columns (Thermo Scientific, product # 89889) at 1,700 x g for 2min.

#### **5.4.2 Colorimetric assay**

A colorimetric Lactate Assay kit purchased from Sigma Aldrich (Catalog Number MAK064) was used to generate a standard curve and to analyze the lactate concentration in media obtained from cell culture. The absorbance was then measured at 570nm using Nanodrop 2000 (Thermo Scientific). The absorbance values were then converted into the concentration of lactate using a generated standard curve.

#### **5.4.3 Biosensor experiments**

This test was conducted in the cell culture media previously obtained. The current was measured with a PPy modified electrode using the GPES software and AUTOLAB system at -0.2V for 120s. The current readings were then applied to the bench top curve of concentration vs. current to determine the concentration of lactate in the media using the biosensor. The accuracy of the device compared to the colorimetric assay was then calculated.

# Chapter 6

## Results



## 6.1 Film Characterization

### 6.1.1 Contact Angle Analysis

Contact angle results showed that the deposited PPy film with embedded LOx enzyme exhibited a contact angle of  $41.6^\circ \pm 8.4$  for  $n=3$ . This contrasts contact angle data obtained for a clean GC electrode, serving as the control, which was  $85^\circ \pm 4.1$  for  $n=3$ . Table 7 below shows the data obtained from these experiments. Figure 24 shows a representative image of the contact angle from a clean electrode and from a PPy-modified electrode.

**Table 7: Contact Angle Analysis Results.**

Sample	Trial 1	Trial 2	Trial 3	Average
Control	84.7	86.6	85.2	85.8
PPy Film	38.8	51.1	35	41.6

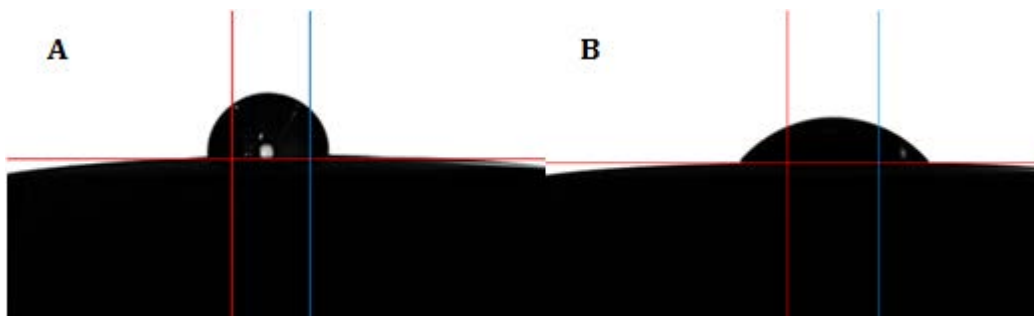


**Figure 27: Contact angles of a (A) clean electrode and a (B) PPy film embedded with LOx. The first image shows a hydrophobic surface while the second is more hydrophilic.**

### 6.1.2 Cyclic Voltammetry

Figure 28 shows the results of the cyclic voltammetry testing. The maximum point on the curve of the electrode coated with PPy/LOx film only increased by  $1.5 \times 10^{-5}$  A while the minimum point only decreased by  $3 \times 10^{-5}$  A.

## 6.2 Bench biosensor validation

### 6.2.1 Lactate Amperometry

The results of the lactate submersion, shown below in Figure 25, illustrate the averages from the three lactate submersion tests. The 500nM concentration shows the smallest system output response while the 1mM exhibits the largest system output response.

The point at which the current levels off for each of the tested concentrations in the lactate amperometry test was plotted against the concentration values to obtain a linear curve. This graph of current vs. concentration can be seen below in Figure 30.

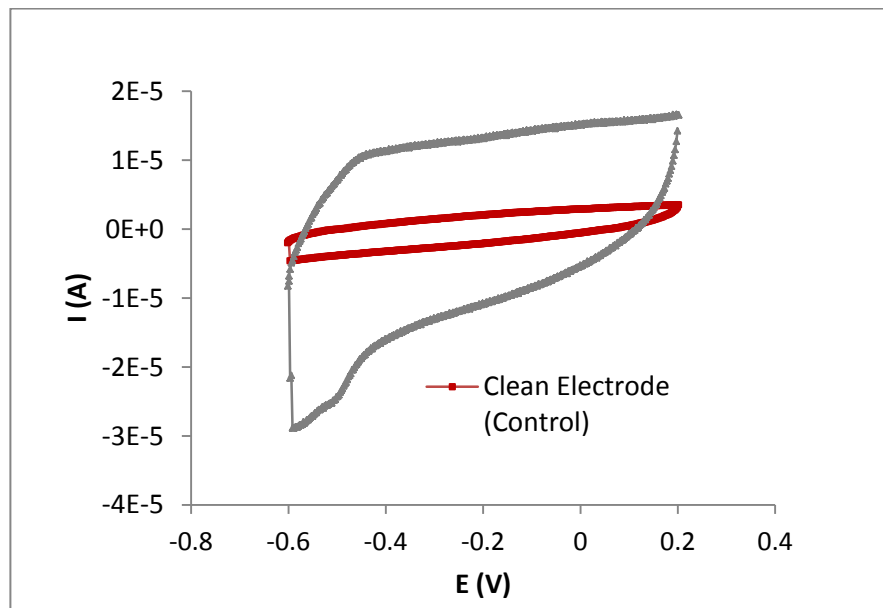


**Figure 28: Cyclic voltammetry results show minimal impedance of electron flow through the film.**

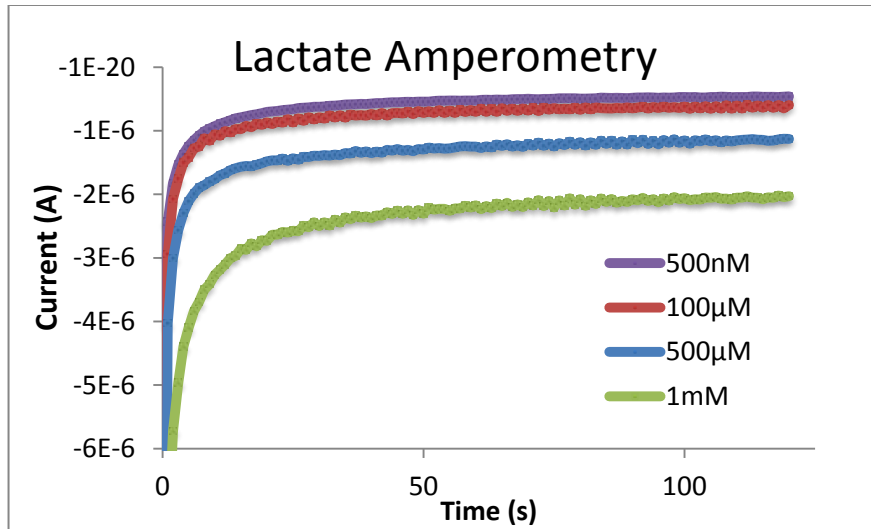


**Figure 29: Change in system output over time after biosensor submersion in various concentrations of lactate. Averages of n=3 are displayed. As the system output increases, the lactate concentration increases proportionally.**

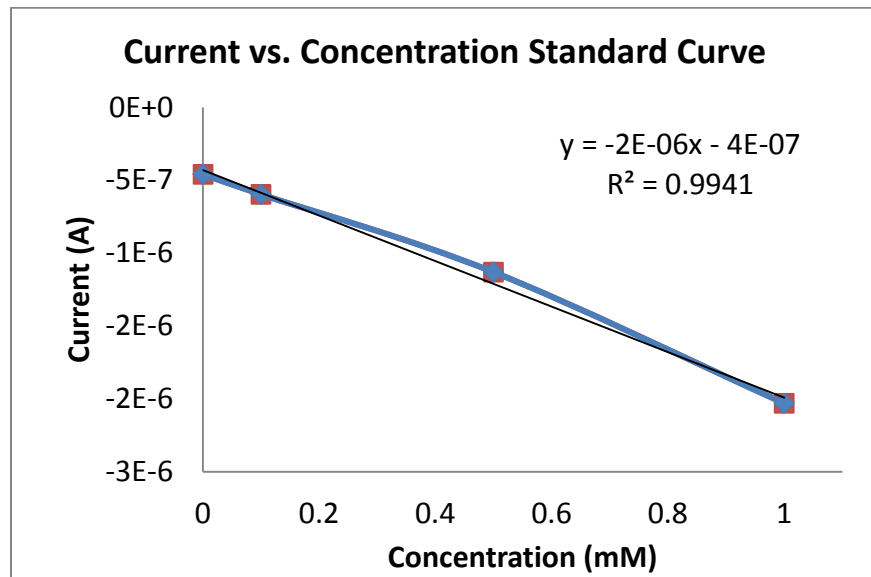


**Figure 30: The increase in system response is directly proportional to increase in current.**

### 6.2.2 Real-time Lactate Recognition

The increasing step-like curve created upon increasing the lactate concentration can be seen in Figure 31.

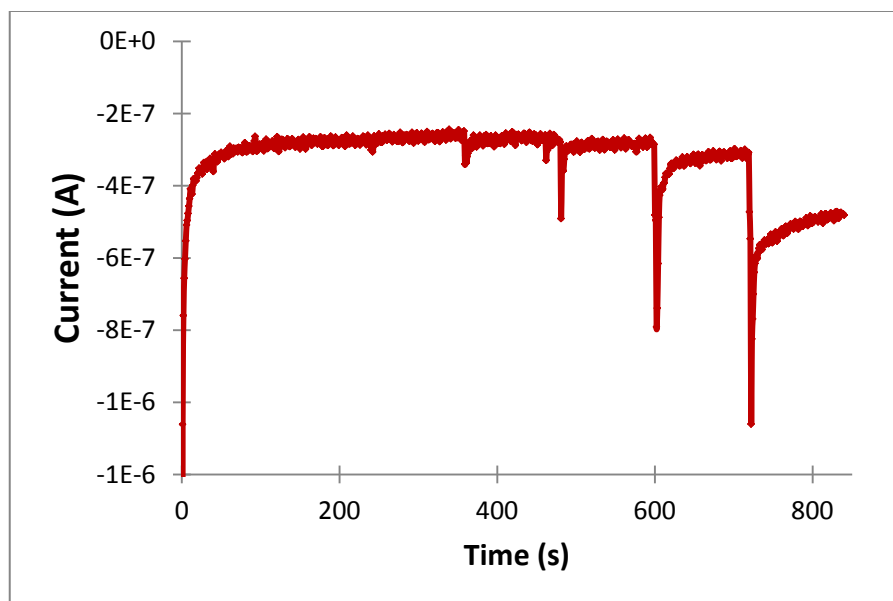


**Figure 31: Real-time recognition of increasing lactate concentrations via stepwise addition. There is an instantaneous response in the output response of the system as the concentration increases. Averages of n=3 are shown.**

### 6.3 *In Vitro* Biosensor Validation

#### 6.3.1 Colorimetric Assay

Using the colorimetric lactate assay, a standard curve of absorbance vs. concentration of lactate at a wavelength of 570nm was generated. The assay was then performed on the collected cell culture media, and the standard curve was used to correlate the resulting absorbances to determine the levels of lactate in media of the respective cell densities. The resulting curve of lactate concentration in media vs. cell density displayed linear behavior and can be seen in Figure 32.

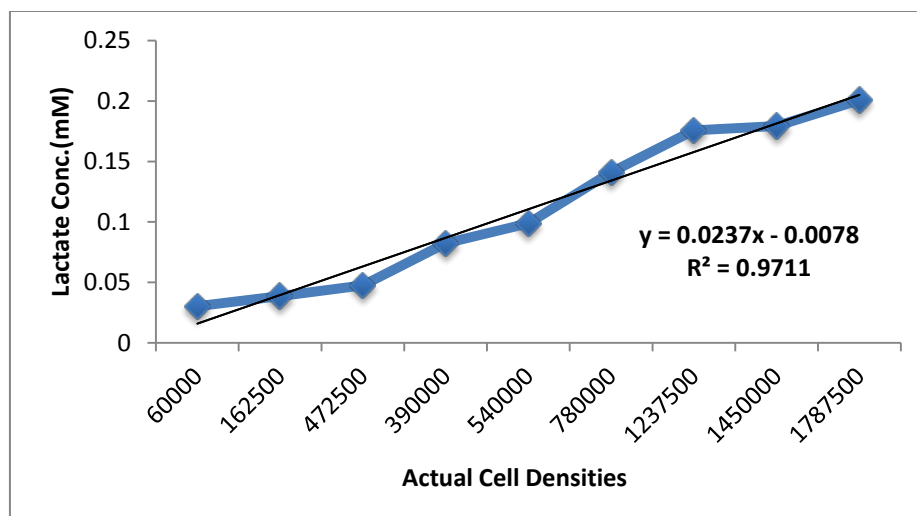


**Figure 32: The graph above shows the curve of lactate concentration in media vs. cell density.**

### 6.3.2 In Media

The results of the biosensor validation testing in media compared to the results using the assay can be seen in Table 8. To determine the accuracy of each test in different cell media, the readings were averaged together. The variance between the values was calculated as a percent difference of 5.4%.

**Table 8: The table below displays the lactate concentrations obtained using the biosensor in media from various cell densities**

Cell Densities	Assay Lactate Concentration (nM)	Biosensor Lactate Concentration (nM)
<b>1,250,000</b>	179	171
<b>1,500,00</b>	200	188

# **Chapter 7**

## **Discussion**

## 7.1 Design Validation

Contact angle analysis showed that the film was present on the surface of the electrode after electrochemical deposition and that it was hydrophilic as expected due to the nature of the PPy. Cyclic voltammetry results showed that compared to the control electrode, the coated electrode experienced minimal increase in its working area, defined as the area between the curves. This means that the electrons were minimally impeded when traveling through the PPy film thus verifying the conductive nature of PPy. From the bench biosensor validation testing the performance of the biosensor was validated. The final results of the lactate amperometry test verified that the increase of output response is directly proportional to the increase in concentration, which validates that this system is applicable for measuring metabolite changes in GBM patients. The results of the real-time lactate recognition test indicate that as the concentration of lactate increases, there is an instantaneous response in which the system output increases proportionally. These tests also show that the sensitivity of the system is on the nM scale which allows it to operate effectively within physiological conditions. Based on the previously reported studies, the systemic lactate levels are on the mM scale, showing our system exceeds the sensitivity requirement to be able to monitor GBM.

After comparing the results of the colorimetric lactate assay kit and the biosensor readings from the same media, the accuracy of the system was determined to be 94.6% allowing for confident GBM monitoring. Because the system detected a change in the levels of lactate produced from only 250,000 cells, the biosensor allows for a more effective monitoring method compared to the available techniques such as MRI and CT scans, which are effective on the order of millions of cells.

## 7.2 Project Considerations

### 7.2.1 Economy

Cancer is among the 10 most expensive medical conditions. The total costs associated with diagnostics, treatment and monitoring of cancer in the U.S. amounted to \$125 billion in 2010 and is projected to reach \$158 billion in 2020 [29]. About 40% of the costs are comprised of monitoring patients over time through frequent hospital exams and laboratory tests[29]. The implantable biosensor system offers a technology that will result in substantial reductions in cost, because it reduces the need for both hospital visits and laboratory tests. The device is designed to supply real-time, accurate data on the progression of the disease and effectiveness of treatments. It not only gives quicker detection of physiological changes associated with tumor return or progression but it also eliminates the economic burden that comes with frequent MRIs, CT scans or blood tests, which are currently performed to monitor patients.

The primary costs associated with the biosensor consist of the cost of surgery needed to implant the device in the patient's body as well as the cost of manufacturing of the electrode, coating and wireless transmission device. These are one-time costs which are expected to amount to a total of approximately \$30,000 per patient. This is only a fraction of the expenses that are associated with monitoring the condition currently thus it is expected that the technology will revolutionize the care for glioblastoma patients and cancer patients in general. This will have a great impact on the healthcare economy. By reducing the cost of monitoring cancer patients this technology will allow more funds to be put into the research and development of personalized treatments for patients, thus improving their chance of survival.



### **7.2.2 Environment**

The biosensor technology greatly reduces the need for CT scans, MRIs and thus allowing for a decreased in the utilization of electricity. The wireless transmitter which will collect the data from the biosensor will be battery operated which overall will result in a reduction in natural resources.

### **7.2.3 Social influence**

The purpose of this study offers a better alternative in monitoring the progression of glioblastoma and will ultimately improve the 2% survival rate after treatment. The implantable biosensor will provide real time *in vivo* efficacy, and therefore will increase patient quality of life as it will eliminate mandatory doctor's visits as well as decrease the patient exposure to radiation. The physician can monitor the cancer from the data wirelessly received from the device. The biosensor itself does not pose any social implications.

### **7.2.4 Ethics**

The main ethical concern for this project is the location of the cancer, the brain. The current method of treating Glioblastoma Multiforme often involves using invasive techniques such as surgery in order to remove the tumor. The long term goal of this device is to make the biosensor implantable and thus animal models will be needed to complete the device verification. Also this project is a first generation study, meaning there isn't much research conducted on designing a biosensor for monitoring cancer; however, the results of this study will positively impact future studies of this device.

### **7.2.5 Health and Safety**

All materials and components used to create the designed biosensor system are fit for use within a human patient. The polypyrrole, if sterilized properly, is biocompatible, the

lactate oxidase enzyme is already found inside the body, and the glassy carbon can be safely used *in vivo*. However, as currently designed without any miniaturization, the biosensor system would be unfit for implantation due to the relatively large size of the electrodes used as well as the uncontained wires used to transfer current through the three electrodes. Although only used to validate the system prior to miniaturization, this system would have significant potential to cause patient harm and discomfort if used as is.

#### **7.2.6 Manufacturability**

The designed biosensor system would be relatively easy to manufacture on a large scale. It only requires one solution and the three electrodes and is completed in 30 minutes. Chemical companies already possess equipment to manufacture and handle large quantities of reagents which similarly be used to create and store the KCl mixture. The largest issue that could arise in respect to manufacturing would be proper storage and handling of the lactate oxidase. This, as with all enzymes, must be stored at sub-freezing temperatures to protect against denaturing and care must be taken to limit freeze/thaw cycles of the enzyme. After being manufactured, the film must be kept hydrated until use, which would not pose any difficulties.

# **Chapter 8**

## **Conclusion and Future Recommendations**

The completion of this project yielded a validated prototype of a polymer film coated electrode for a biosensor system. The results obtained through validation testing allowed us to make recommendations for future iterations of this design.

## 8.1 Conclusions

Testing of the final prototype yielded three main conclusions:

### **1. The initial theory behind the prototype design was valid.**

The success of our prototype design hinged on the ability of the PPy film to be deposited using electrochemical deposition, the LOx to be immobilized through electrostatic interactions while still being capable of functioning to break down lactate into hydrogen peroxide, the hydrogen peroxide naturally breaking down at a rate fast enough to measure lactate concentration, and free electrons being conducted through the PPy film to the surface of the electrode. The testing showed that all necessary steps were occurring as theorized, which allows for optimization of each component in the future.

### **2. The design was a valid solution to the issues presented in the client statement.**

The final design met the basic requirements of the client statement to develop a biosensor system that could selectively bind to an overexpressed metabolite in GBM and determine the changes in this concentration in real-time. Our prototype achieved each of these requirements, allowing for it to be utilized, after future iterations, for the application of monitoring in real-time the response of GBM to a therapeutic regimen.

### **3. Building up our prototype to include all elements of the final design will achieve a more optimal system.**

Since our results validated the fundamental mechanism by which the system operates, it can now be built up so that all components of the final design can be

incorporated. This will allow for the optimization of the capabilities of the overall system, allowing for it to ultimately be utilized as an implantable system that can be validated *in vivo*.

## **8.2 Measure Glutamate Levels**

The first recommendation for future iterations of the design is to expand the biorecognition system biosensor system to be able to monitor the levels of glutamate in addition to the levels of lactate. While the increased expression of lactate is a normal metabolic change for most types of cancer, elevated glutamate levels are more specific to brain cancer, including GBM. By measuring the levels of this metabolite, the system will be more efficient at detecting the response of GBM to treatment. To incorporate this, a second working electrode could be created using the same methods outlined in this report, but using glutamate oxidase (GLOx) for the enzyme instead of LOx. This second working electrode would monitor levels of glutamate while the first measures the levels of lactate, creating a more comprehensive system.

## **8.3 Incorporate Horseradish Peroxidase**

In order to increase the sensitivity while decreasing the response time of the system, Horseradish Peroxidase (HRP) enzyme should be incorporated alongside the LOx enzyme in the PPy film. This enzyme serves to catalyze the breakdown of H<sub>2</sub>O<sub>2</sub> into free electrons much faster than what naturally occurs through reduction via the applied current. This would allow the recognition of lactate in the environment to occur faster, as well as break down H<sub>2</sub>O<sub>2</sub> that may escape the system prior to being broken down, serving to increase the biosensor's capabilities.

#### **8.4 Add Outer Chitosan Layer**

The addition of a non-conductive, porous chitosan (CHI) film layered on top of the PPy film would serve to improve the sensitivity as well as the selectivity of the system. This layer would serve to trap free electrons generated by the breakdown of H<sub>2</sub>O<sub>2</sub>, as well as protect against the introduction of unwanted outside molecules into the system. The team began preliminary testing of introducing a CHI film, but further testing is necessary to introduce this component of the biosensor.

#### **8.5 Miniaturize Electrode System**

After all components are introduced into the system and the completed biosensor is validated, it needs to be miniaturized. This requires the use of a three-electrode array onto which the same manufacturing methods can be applied to produce a PPy and CHI film. This miniaturization will allow for the initiation of in vivo testing of the system, where the use of the biosensor can be optimized and further validated.

# References

1. Stupp, R., et al., *Promising survival for patients with newly diagnosed glioblastoma multiforme treated with concomitant radiation plus temozolomide followed by adjuvant temozolomide*. J Clin Oncol, 2002. **20**(5): p. 1375-82.
2. Lee, J., *Meningiomas: Diagnosis, Treatment, and Outcome* 2009: Springer
3. Ohgaki, H., et al., *Genetic pathways to glioblastoma: a population-based study*. Cancer Res, 2004. **64**(19): p. 6892-9.
4. DeAngelis, L., *Brain Tumors* The New England Journal of Medicine 2001. **344**(2): p. 114-123.
5. Galanis, E., et al., *Phase II trial of temsirolimus (CCI-779) in recurrent glioblastoma multiforme: a North Central Cancer Treatment Group Study*. J Clin Oncol, 2005. **23**(23): p. 5294-304.
6. Pelletier, G., et al., *Quality of life in brain tumor patients: the relative contributions of depression, fatigue, emotional distress, and existential issues*. J Neurooncol, 2002. **57**(1): p. 41-9.
7. Reardon, D.A., et al., *Recent advances in the treatment of malignant astrocytoma*. J Clin Oncol, 2006. **24**(8): p. 1253-65.
8. Yuile, P., et al., *Survival of glioblastoma patients related to presenting symptoms, brain site and treatment variables*. J Clin Neurosci, 2006. **13**(7): p. 747-51.
9. Berger, A., *Magnetic resonance imaging*. BMJ, 2002. **324**(7328): p. 35.
10. Tancredi, L.R. and J.D. Brodie, *The brain and behavior: limitations in the legal use of functional magnetic resonance imaging*. Am J Law Med, 2007. **33**(2-3): p. 271-94.
11. Dilsizian, V.a.P., G., *Cardiac CT, PET and MR* 2010, Hoboken, NJ: Wiley-Blackwell 386.
12. Lawson, H.C., et al., *Interstitial chemotherapy for malignant gliomas: the Johns Hopkins experience*. J Neurooncol, 2007. **83**(1): p. 61-70.
13. Harrison, L.B., et al., *Impact of tumor hypoxia and anemia on radiation therapy outcomes*. Oncologist, 2002. **7**(6): p. 492-508.
14. Mehta, M.P., W.A. Tome, and G.H. Olivera, *Radiotherapy for brain tumors*. Curr Oncol Rep, 2000. **2**(5): p. 438-44.
15. Vander Heiden, M.G., L.C. Cantley, and C.B. Thompson, *Understanding the Warburg effect: the metabolic requirements of cell proliferation*. Science, 2009. **324**(5930): p. 1029-33.
16. Marie, S.K. and S.M. Shinjo, *Metabolism and brain cancer*. Clinics (Sao Paulo), 2011. **66 Suppl 1**: p. 33-43.
17. Wolf, A., S. Agnihotri, and A. Guha, *Targeting metabolic remodeling in glioblastoma multiforme*. Oncotarget, 2010. **1**(7): p. 552-62.
18. Broer, S. and N. Brookes, *Transfer of glutamine between astrocytes and neurons*. J Neurochem, 2001. **77**(3): p. 705-19.
19. Hall, C.N., et al., *Oxidative phosphorylation, not glycolysis, powers presynaptic and postsynaptic mechanisms underlying brain information processing*. J Neurosci, 2012. **32**(26): p. 8940-51.
20. Jones, R.G. and C.B. Thompson, *Tumor suppressors and cell metabolism: a recipe for cancer growth*. Genes Dev, 2009. **23**(5): p. 537-48.
21. Bayley, J.P. and P. Devilee, *The Warburg effect in 2012*. Curr Opin Oncol, 2012. **24**(1): p. 62-7.
22. Lunt, S.Y. and M.G. Vander Heiden, *Aerobic glycolysis: meeting the metabolic requirements of cell proliferation*. Annu Rev Cell Dev Biol, 2011. **27**: p. 441-64.



23. Dang, C.V., *Glutaminolysis: supplying carbon or nitrogen or both for cancer cells?* Cell Cycle, 2010. **9**(19): p. 3884-6.
24. DeBerardinis, R.J., et al., *Beyond aerobic glycolysis: transformed cells can engage in glutamine metabolism that exceeds the requirement for protein and nucleotide synthesis.* Proc Natl Acad Sci U S A, 2007. **104**(49): p. 19345-50.
25. Noch, E. and K. Khalili, *Molecular mechanisms of necrosis in glioblastoma: the role of glutamate excitotoxicity.* Cancer Biol Ther, 2009. **8**(19): p. 1791-7.
26. Keusgen, M., *Biosensors: new approaches in drug discovery.* Naturwissenschaften, 2002. **89**(10): p. 433-44.
27. Arya, S.K., et al., *Recent advances in ZnO nanostructures and thin films for biosensor applications: review.* Anal Chim Acta, 2012. **737**: p. 1-21.
28. Wang, J., *Electrochemical biosensors: towards point-of-care cancer diagnostics.* Biosens Bioelectron, 2006. **21**(10): p. 1887-92.
29. Marchione, M., *Cancer's growing burden: the high cost of care.*, in Associated Press 2012
30. Zhou, G.J.e.a., *Reagentless Chemiluminescence Biosensor for Determination of Hydrogen Peroxide Based on the Immobilization of Horseradish Peroxidase on Biocompatible Chitosan Membrane.* Sensors and Actuators B: Chemical, 2002. **81**(2-3): p. 334-339.
31. Castillo, J., et al., *Bienzyme biosensors for glucose, ethanol and putrescine built on oxidase and sweet potato peroxidase.* Biosens Bioelectron, 2003. **18**(5-6): p. 705-14.
32. Kotanen, C.N., et al., *Implantable enzyme amperometric biosensors.* Biosens Bioelectron, 2012. **35**(1): p. 14-26.
33. Vaddiraju, S., et al., *Emerging synergy between nanotechnology and implantable biosensors: a review.* Biosens Bioelectron, 2010. **25**(7): p. 1553-65.
34. Thevenot, D.R., et al., *Electrochemical biosensors: recommended definitions and classification.* Biosens Bioelectron, 2001. **16**(1-2): p. 121-31.
35. Raba, J.M., H., *Glucose Oxidase as an Analytical Reagent.* Analytical Chemistry, 1995. **25**(1): p. 1-42.
36. O'Neill, R.D., et al., *Comparisons of platinum, gold, palladium and glassy carbon as electrode materials in the design of biosensors for glutamate.* Biosens Bioelectron, 2004. **19**(11): p. 1521-8.
37. Wilson, G.S. and R. Gifford, *Biosensors for real-time in vivo measurements.* Biosens Bioelectron, 2005. **20**(12): p. 2388-403.
38. De Benedetto, G.E.F., F.; Zamboni, P.G., *One-step fabrication of a bienzyme glucose sensor based on glucose oxidase and peroxidase immobilized onto a poly(pyrrole) modified glassy carbon electrode.* Biosensors and Bioelectronics, 1996. **11**(10): p. 1001-1008.
39. Lindgren, A., et al., *Biosensors based on novel peroxidases with improved properties in direct and mediated electron transfer.* Biosens Bioelectron, 2000. **15**(9-10): p. 491-7.
40. Gajovic, N., et al., *Operation of a miniature redox hydrogel-based pyruvate sensor in undiluted deoxygenated calf serum.* Anal Chem, 2000. **72**(13): p. 2963-8.
41. Fabre, B.B., S.; Cespuoglio, G., *Voltammetric detection of NO in the rat brain with an electronic conducting polymer and Nafion® bilayer-coated carbon fibre electrode.* Journal of Electroanalytical Chemistry, 1997. **426**(1-2): p. 75-83.

42. Gajovic, N.H., K.; Warsinke, A.; Schuhmann, W.; Scheller, F.W., *A Pyruvate Oxidase Electrode Based on an Electrochemically Deposited Redox Polymer*. *Electroanalysis*, 1999. **11**: p. 1377-1383.
43. Clark, R.A.Z., S.E.; Ewing, A.G., *Electrochemistry in neuronal microenvironments* *Electroanalytical Chemistry*, 1998. **20**: p. 227-294.
44. Bharathi, S. and M. Nogami, *A glucose biosensor based on electrodeposited biocomposites of gold nanoparticles and glucose oxidase enzyme*. *Analyst*, 2001. **126**(11): p. 1919-22.
45. Somasundrum, M.T., M; Kirtikara, K., *H<sub>2</sub>O<sub>2</sub> from an oxidase enzyme can be detected cathodically using metal microparticles dispersed in a polymeric film electrode*. *Journal of Electroanalytical Chemistry*, 1996. **407**(1-2): p. 247-251.
46. Welch, C.M., et al., *Silver nanoparticle assemblies supported on glassy-carbon electrodes for the electro-analytical detection of hydrogen peroxide*. *Anal Bioanal Chem*, 2005. **382**(1): p. 12-21.
47. Mateo, C.P., J.; Fernandez-Lorente, G.; Guisan, J.; Fernandez-Lafuente, R., *Improvement of enzyme activity, stability and selectivity via immobilization techniques*. *Enzyme and Microbial Technology*, 2007. **40**(6): p. 1451-1463.
48. El Nashar, R.M., *Flow injection catalase activity measurement based on gold nanoparticles/carbon nanotubes modified glassy carbon electrode*. *Talanta*, 2012. **96**: p. 161-7.
49. Ibupoto, Z.H., et al., *Electrochemical L-lactic acid sensor based on immobilized ZnO nanorods with lactate oxidase*. *Sensors (Basel)*, 2012. **12**(3): p. 2456-66.
50. Unnikrishnan, B., S. Palanisamy, and S.M. Chen, *A simple electrochemical approach to fabricate a glucose biosensor based on graphene-glucose oxidase biocomposite*. *Biosens Bioelectron*, 2013. **39**(1): p. 70-5.
51. Wisniewski, N. and M. Reichert, *Methods for reducing biosensor membrane biofouling*. *Colloids Surf B Biointerfaces*, 2000. **18**(3-4): p. 197-219.
52. Lindner, E.T., K.; Pungor, E., *Definition and determination of response time of ion selective electrodes*. *Pure Applied Chemistry*, 1986. **58**(3): p. 469-479.
53. Davis, F.a.H., S., *Polymers in biosensors*, in *Biomedical Polymers*, M. Jenkins, Editor 2007, Woodhead Publishing.
54. Arshak, K., Velusamy, V., Korostynska, O, Oliwa-Stasiak, K, and Adley, C., *Conducting Polymers and Their Applications to Biosensors: Emphasizing on Foodborne Pathogen Detection*. *Sensors Journal*, 2009. **9**(12): p. 1942-1951.
55. Gough, D.A., J.Y. Lucisano, and P.H. Tse, *Two-dimensional enzyme electrode sensor for glucose*. *Anal Chem*, 1985. **57**(12): p. 2351-7.
56. McShane, M., *Nanofilms as Universal Coatings for Biosensors*. *Sensors Conference*, 2009. **1**: p. 1208-1211.
57. Sotiropoulou, S.V., V.; Chaniotakis, N., *Stabilization of Enzymes in Nanoporous Materials for Biosensor Applications*. *Analytical Chemistry*, 2008. **Crete**(Grece).
58. Stoytcheva, M.e.a., *Analytical Characteristics of Electrochemical Biosensors*. *Portugaliae Electrochemica Acta*, 2009. **27**(3): p. 353-362.
59. Chae, K.H.e.a., *Anti-fouling epoxy coatings for optical biosensor application based on phosphorylcholine*. *Sensors and Actuators B: Chemical*, 2007. **124**: p. 153-160.
60. Gerard, M., A. Chaubey, and B.D. Malhotra, *Application of conducting polymers to biosensors*. *Biosens Bioelectron*, 2002. **17**(5): p. 345-59.

61. Shirakawa, H.e.a., *Synthesis of electrically conducting organic polymers: halogen derivatives of polyacetylene*. Journal of the Chemical Society, Chemical Communications, 1977(16): p. 578-580.
62. Nita, A.M., *Conducting polymers in Biosensors: A Review*. Universitatea Stefan cel Mare Suceava, 2010. **2**(1).
63. Chen, F. and P. Liu, *Conducting polyaniline nanoparticles and their dispersion for waterborne corrosion protection coatings*. ACS Appl Mater Interfaces, 2011. **3**(7): p. 2694-702.
64. Santhanam, K., *Conducting Polymer for Biosensors: Rationale Based on Models*. Pure and Applied Chemistry, 1998. **70**(6): p. 1256-1262.
65. Malhotra, B.D., A. Chaubey, and S.P. Singh, *Prospects of conducting polymers in biosensors*. Anal Chim Acta, 2006. **578**(1): p. 59-74.
66. Qu, F., et al., *Amperometric biosensor for choline based on layer-by-layer assembled functionalized carbon nanotube and polyaniline multilayer film*. Anal Biochem, 2005. **344**(1): p. 108-14.
67. Guven, O., *Radiation-induced conductivity control in polyaniline blends/composites*. Radiation Physics and Chemistry, 2007. **76**(8-9): p. 1302-1307.
68. Ateh, D.D., H.A. Navsaria, and P. Vadgama, *Polypyrrole-based conducting polymers and interactions with biological tissues*. J R Soc Interface, 2006. **3**(11): p. 741-52.
69. Uang, Y.M. and T.C. Chou, *Fabrication of glucose oxidase/polypyrrole biosensor by galvanostatic method in various pH aqueous solutions*. Biosens Bioelectron, 2003. **19**(3): p. 141-7.
70. Nakabayashi, Y.e.a., *Amperometric glucose sensors fabricated by electrochemical polymerization of phenols on carbon paste electrodes containing ferrocene as electron transfer mediator*. Analytical Science, 1998. **14**: p. 1069-1077.
71. Nakabayashi, Y.a.Y., H., *Amperometric biosensors for sensing of hydrogen peroxide based on electron transfer between horseradish peroxidase and ferrocene as a mediator*. Analytical Science, 2000. **16**: p. 609-613.
72. Kingshott, P.a.G., H.J., *Surfaces that resist bioadhesion*. Current Opinion in Solid State & Materials Science, 1999. **4**(4): p. 403-412.
73. Bridges, A.W. and A.J. Garcia, *Anti-inflammatory polymeric coatings for implantable biomaterials and devices*. J Diabetes Sci Technol, 2008. **2**(6): p. 984-94.
74. Yan, J., et al., *Enzyme-containing hydrogel micropatterns serving a dual purpose of cell sequestration and metabolite detection*. Biosens Bioelectron, 2009. **24**(8): p. 2604-10.
75. Ziegler, W.e.a., *Agar-Supported Lipid Bilayers- Basic Structures for Biosensor Design*. Colloids and Surfaces A: Physicochemical and Engineering Aspects, 1998. **140**(1-3): p. 357-367.
76. Mousty, C.e.a., *Fabrication of Organic Phase Biosensor Based on Multilayered Polyphenol Oxidase Protected by an Alginate Coating*. Electrochemistry Communications, 2001. **3**(12): p. 727-732.
77. Che, X., et al., *A glucose biosensor based on chitosan-Prussian blue-multiwall carbon nanotubes-hollow PtCo nanochains formed by one-step electrodeposition*. Colloids Surf B Biointerfaces, 2011. **84**(2): p. 454-61.

78. Wang, G., et al., *Amperometric hydrogen peroxide biosensor with sol-gel/chitosan network-like film as immobilization matrix*. Biosens Bioelectron, 2003. **18**(4): p. 335-43.
79. Magalhaes, J.M. and A.A. Machado, *Urea potentiometric biosensor based on urease immobilized on chitosan membranes*. Talanta, 1998. **47**(1): p. 183-91.
80. Miao, Y.a.T., S., *Amperometric hydrogen peroxide biosensor with silica sol-gel/chitosan film as immobilization matrix*. Analytica Chimica Acta, 2001. **437**(1): p. 87-93.
81. Miao, Y.e.a., *Amperometric Glucose Biosensor Based on Immobilization of Glucose Oxidase in Chitosan Matrix Cross-Linked With Glutaraldehyde*. Electroanalysis, 2001. **13**(4): p. 347-349.
82. Chen, X.J., J.; and Dong, S., *Organically Modified Sol-Gel/Chitosan Composite Based Glucose*. Electroanalysis, 2003. **15**(7): p. 608-612.
83. Cruz, J., M. Kawasaki, and W. Gorski, *Electrode coatings based on chitosan scaffolds*. Anal Chem, 2000. **72**(4): p. 680-6.
84. Bao, S. and T. Nomura, *Silver-selective sensor using an electrode-separated piezoelectric quartz crystal modified with a chitosan derivative*. Anal Sci, 2002. **18**(8): p. 881-5.
85. Wan, Y.e.a., *Synthesis, Characterization and Ionic Conductive Properties of Phosphorylated Chitosan Membranes*. Macromolecular Chemistry and Physics, 2003. **204**: p. 850-858.
86. Wang, H.S.P., Q.X and Wang, G.X, *A Biosensor Based on Immobilization of Horseradish Peroxidase in Chitosan Matrix Cross-linked with Glyoxal for Amperometric Determination of Hydrogen Peroxide*. Sensors and Actuators B: Chemical, 2005. **5**: p. 266-276.
87. Wei, X., J. Cruz, and W. Gorski, *Integration of enzymes and electrodes: spectroscopic and electrochemical studies of chitosan-enzyme films*. Anal Chem, 2002. **74**(19): p. 5039-46.
88. Genta, I.e.a., *Influence of Glutaraldehyde on Drug Release and Mucoadhesive Properties of Chitosan Microspheres*. Carbohydrate Polymers, 1998. **36**(2-3): p. 81-88.
89. Baba, Y., et al., *Preparation of chitosan derivatives containing methylthiocarbamoyl and phenylthiocarbamoyl groups and their selective adsorption of copper(II) over iron(III)*. Anal Sci, 2002. **18**(3): p. 359-61.
90. Modrzejewska, Z.a.K., W., *Separation of Cr (VI) on Chitosan Membranes*. Industrial and Engineering Chemistry Research, 1999. **38**: p. 4946-4950.
91. Sriyudthsak, M.Y., H.; Moriizumi, T;, *Enzyme-immobilized Langmuir-Blodgett film for a biosensor*. Thin Solid Films, 1988. **10**(1-2): p. 463-469.
92. Sharma, S.K., et al., *Biosensor based on Langmuir-Blodgett films of poly(3-hexyl thiophene) for detection of galactose in human blood*. Biotechnol Lett, 2004. **26**(8): p. 645-7.
93. Roberts, G., *Langmuir-Blodgett Films*, ed. 11990: Springer. 444.
94. Peterson, R.I., *Langmuir-Blodgett Films*. Journal of Applied Physics, 1990. **23**(4).
95. Du, Y., et al., *Layer-by-layer electrochemical biosensor with aptamer-appended active polyelectrolyte multilayer for sensitive protein determination*. Biosens Bioelectron, 2010. **25**(8): p. 1902-7.

96. Lin, H.e.a., *Layer-by-layer self-assembly of in situ polymerized polypyrrole on sulfonated poly(arylene ether ketone) membrane with extremely low methanol crossover*. International Journal of Hydrogen Energy, 2009. **34**(24): p. 9795-9801.
97. Fou, A.C.a.R., M.F, *Molecular-Level Processing of Conjugated Polymers and Layer-by-Layer Manipulation of In-Situ Polymerized p-type Doped Conducting Polymer*. Macromolecules, 1995. **28**: p. 7115-7120.
98. Zheng, S.e.a., *Self-assembly and Characterization of Polypyrrole and Polyallylamine Multilayer Films and Hollow Shells*. Chemistry of Materials, 2004. **16**(19): p. 3677-3781.
99. Weinheim, K., *Growth of Polypyrrole-like Films on Self-Assembly Nanostructured Silicon Surfaces by PECVD*. Chemical Vapor Deposition, 2009. **15**(4-6): p. 128-132.
100. Vercelli, B.a.Z., G, *Polypyrrole Self-Assembled Monolayers and Electrostatically Assembled Multilayers on Gold and Platinum Electrodes for Molecular Junctions*. Chemistry of Materials, 2006. **18**(16): p. 3754-3763.
101. Park, S.e.a., *Self-assembly of Meoscopic Metal-Polymer Amphiphiles*. Science Magazine, 2004. **303**.
102. Iost, R.e.a., *Strategies of Nano-Manipulation for Application in Electrochemical Biosensors*. International Journal of Electrochemical Science, 2011. **6**: p. 2965-2997.
103. Yang, X.D., T. and Lu, Y., *Synthesis of novel sunflower-like silica/polypyrrole nanocomposites via self-assembly polymerization*. Polymer, 2006. **47**(1): p. 441-447.
104. Fou, A.C., *Design, Fabrication and Characterization of Complex, Multilayer Heterostructures of Conjugated and Non-conjugated Polymers via Molecular Self-Assembly*. Department of Materials Science and Engineering, 1995. **Massachusetts Institute of Technology, Doctoral Thesis**
105. So, H.M.e.a., *Single-Walled Carbon Nanotube Biosensors Using Aptamers as Molecular Recognition Elements*. Journal of American Chemical Society, 2005. **127**(34): p. 11906-11907.
106. Huang, J.e.a., *Multi-walled carbonnanotubes-based glucose biosensor prepared by a layer-by-layer technique*. Materials Scence and Engineering, 2006. **26**(1): p. 113-117.
107. Jain, K.K., *Nanodiagnosics: application of nanotechnology in molecular diagnostics*. Expert Rev Mol Diagn, 2003. **3**(2): p. 153-61.
108. Lin, Y., ; Lu, F.; and Ren, Z., *Glucose Biosensors Based on Carbon Nanotube Nanoelectrode Ensembles*. NanoLetters, 2003. **4**(2): p. 191-195.
109. Maxwell, D.J., J.R. Taylor, and S. Nie, *Self-assembled nanoparticle probes for recognition and detection of biomolecules*. J Am Chem Soc, 2002. **124**(32): p. 9606-12.
110. Xiao, Y.e.a., *DNA biosensors based on layer-by-layer self-assembled multilayer films of carbon nanotubes and gold nanoparticles*. Proceedings of the Second International Conference on Smart Materials and Nanotechnology in Engineering, 2009. **7493**.
111. Hou, S., et al., *Amperometric acetylcholine biosensor based on self-assembly of gold nanoparticles and acetylcholinesterase on the sol-gel/multi-walled carbon nanotubes/choline oxidase composite-modified platinum electrode*. Biosens Bioelectron, 2012. **33**(1): p. 44-9.
112. Norouzi, P., *Glucose Biosensor Based on MWCNTs-Gold Nanoparticles in a Nafion Film on the Glassy Carbon Electrode Using Flow Injection FFT Continuous Cyclic*

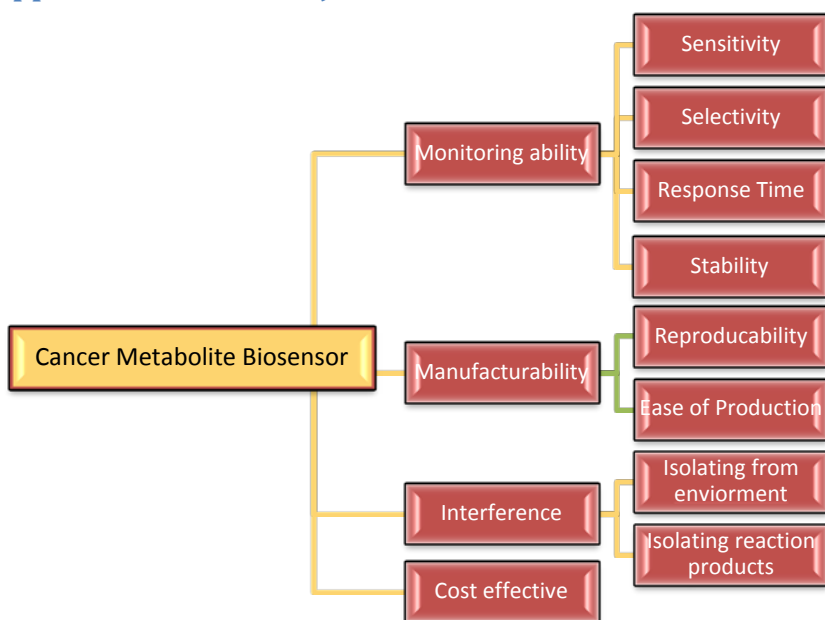
- Voltammetry*. International Journal of Electrochemical Science, 2010. **5**: p. 1213-1224.
113. Wu, B.Y., et al., *Amperometric glucose biosensor based on multilayer films via layer-by-layer self-assembly of multi-wall carbon nanotubes, gold nanoparticles and glucose oxidase on the Pt electrode*. Biosens Bioelectron, 2007. **22**(12): p. 2854-60.
  114. Crespolho, F.N.e.a., *A strategy for enzyme immobilization on layer-by-layer dendrimer-gold nanoparticle electrocatalytic membrane incorporating redox mediator*. Electrochemistry Communications, 2006. **8**: p. 1665-1670.
  115. Wang, C., et al., *A pH-sensitive molecularly imprinted nanospheres/hydrogel composite as a coating for implantable biosensors*. Biomaterials, 2010. **31**(18): p. 4944-51.
  116. Baby, T.T., *Non-Enzymatic Glucose and Cholesterol Biosensors Based on Silica Coated Nano Iron Oxide Dispersed Multiwalled Carbon Nanotubes*. Nanoscience, Technology and Societal Implications (NSTSI), 2011: p. 1-6.
  117. Alhadef, E.a.B., N., *Graphite-Composites Alternatives for Electrochemical Biosensor Metal, Ceramic and Polymeric Composites for Various Uses* 2010.
  118. Bharathi, S.a.L., O. , *Sol-gel-derived nanocrystalline gold-silicate composite biosenso*. Analytical Communications, 1998. **35**: p. 29-31.
  119. Chen, L.X., H and Li, J., *Electrochemical glucose biosensor based on silver nanoparticles/multiwalled carbon nanotubes modified electrode*. Journal of Solid State Electrochemistry, 2012. **16**(10): p. 3323-3329.
  120. Barton, A.C., et al., *Sonochemically fabricated microelectrode arrays for biosensors offering widespread applicability: Part I*. Biosens Bioelectron, 2004. **20**(2): p. 328-37.
  121. Spahn, C.a.M., S., *Enzyme Immobilization in Biotechnology*. Recent Patents on Engineering, 2008. **2**: p. 195-200.
  122. Tsai, M.a.T., Y., *Adsorption of glucose oxidase at platinum-multiwalled carbon nanotube-alumina-coated silica nanocomposite for amperometric glucose biosensor*. Sensors and Actuators B: Chemical, 2009. **141**(2): p. 592-598.
  123. Trevan, M.D., *Enzyme immobilization by adsorption*. Methods Mol Biol, 1988. **3**: p. 481-9.
  124. Debeche, T.e.a., *Structured fiber supports for gas phase biocatalysts*. Enzyme and Microbial Technology, 2005. **36**: p. 911-916.
  125. Brena B., B.-V., F., *Immobilization of Enzymes*, in *Methods in Biotechnology: Immobilization of Enzymes and Cells, 2*, Editor 2006, Humana Press. p. 15-29.
  126. Trevan, M.D., *Enzyme immobilization by covalent bonding*. Methods Mol Biol, 1988. **3**: p. 495-510.
  127. Hanefeld, U., L. Gardossi, and E. Magner, *Understanding enzyme immobilisation*. Chem Soc Rev, 2009. **38**(2): p. 453-68.
  128. Whitcombe, M.J., *Molecularly imprinted polymers: smart hydrogel crystal gardens*. Nat Chem, 2011. **3**(9): p. 657-8.
  129. Huang, H.C., et al., *Photo-lithographically impregnated and molecularly imprinted polymer thin film for biosensor applications*. J Chromatogr A, 2004. **1027**(1-2): p. 263-8.
  130. Whitcombe, M.J.a.V., E.N, *Imprinted Polymers*. Advanced Materials, 2001. **13**(7): p. 467-478.

131. Chen, P.Y., et al., *A novel molecularly imprinted polymer thin film as biosensor for uric acid*. Talanta, 2010. **80**(3): p. 1145-51.
132. Hong, C.C., et al., *A disposable microfluidic biochip with on-chip molecularly imprinted biosensors for optical detection of anesthetic propofol*. Biosens Bioelectron, 2010. **25**(9): p. 2058-64.
133. Yano, K.a.K, I. , *Molecularly Impinted Polymers for Biosensor Applications*. Trends in Analytical Chemistry, 1999. **18**(3): p. 199-204.
134. Alatraktchi, F.A., et al., *Surface area expansion of electrodes with grass-like nanostructures and gold nanoparticles to enhance electricity generation in microbial fuel cells*. Bioresour Technol, 2012. **123**: p. 177-83.
135. Cosnier, S., et al., *An electrochemical method for making enzyme microsensors. Application to the detection of dopamine and glutamate*. Anal Chem, 1997. **69**(5): p. 968-71.
136. Ge, S., et al., *Disposable electrochemical immunosensor for simultaneous assay of a panel of breast cancer tumor markers*. Analyst, 2012. **137**(20): p. 4727-33.
137. Behrens, P.F., et al., *Extracellular glutamate and other metabolites in and around RG2 rat glioma: an intracerebral microdialysis study*. J Neurooncol, 2000. **47**(1): p. 11-22.

# Appendices



**Appendix 3.A: Objectives tree for Cancer Metabolite Biosensor**



**Appendix 3.B: Pairwise comparison chart of the primary objectives.**

	Monitoring ability	Manufacturability	Interference	Cost effectiveness	Total
Monitoring ability		1	1	1	3
Manufacturability	0		1	1	2
Interference	0	0		1	1
Cost effectiveness	0	0	0		0

**Appendix 3.C: Pairwise comparison chart of the secondary objectives.**

	Reproducibility	Sensitivity	Selectivity	Response Time	Stability	Total
Reproducibility		0	0	1	0.5	<b>1.5</b>
Sensitivity	1		0.5	1	1	<b>3.5</b>
Selectivity	1	0.5		1	1	<b>3.5</b>
Response Time	0	0	0		0.5	<b>0.5</b>
Stability	0.5	0	0	1		<b>1.5</b>

**Appendix 4.A: Functions-Means Chart**

Function	Means				
Biorecognition	Enzymes	Ligands	Antigen		
Transduction	Oxidase	Dehydrogenase	Hydrogenase		
Conduction	Nanostructures	Conductive	Porous Non-conductive	Non-conductive w/ Nanostructures	Conductive/ Non-conductive Composite
Signal Processing	Autolab PGSTA12	LabView/ Biopack			

## Appendix 4.B: Material Evaluation

The team decided to rank the specific materials in a pass-fail fashion in each category based on expected performance for each material class. During the evaluation, the only number comparison used was the price of each material, for the rest of the properties the evaluation was based on information found in the literature. The material either received a green check for performing well on the specific criteria or a red check not adequately fulfilling the specific need.

Conductive						
	Biocompatible	Cost (\$/g)	Ease of Synthesis and Processability	Conductivity (S/cm)	Enzyme Immobilization	Stability
Polypyrrole	✓	✗ 21.06	✓ synthesized	✓ 1000	✓ charge	✓
Polyaniline	✓	✓ 10.3	✓ synthesized	✗ 1	✓ crosslinking	✓
Polythiophene	✓	✓ 49.5	✗ non-synthesized	✓ 1000	✗	✓
Non-Conductive						
	Biocompatible	Cost (\$/g)	Ease of Synthesis and Processability	Insulating	Enzyme Immobilization	Stability
Agarose	✓	✗ 0.79	✓	✓	✓	✓
Chitosan	✓	✓ 2.86	✓	✓	✓	✓
PEG	✓	✗ 2.52	✓	✓	✓	✗
Conductive Structures						
	Biocompatible	Cost	Ease of Synthesis and Processability	Conductivity	Enzyme Immobilization	Stability
CNT's	✓	✗ 300	✗	✓	✗	✗
Palladium Nanoparticles	✓	✗ 2000	✓	✓	✗	✗
Gold Nanoparticles	✓	✗ 250	✓	✓	✗	✗

This ranking system was based on the following properties:

- **Biocompatibility:** The biocompatibility of each polymer was determined through a literature review and if the polymer was biocompatible it received a green check mark.
- **Cost:** The cost of each material was explored and the material was then ranked based on the results. After comparing costs, red checks were assigned to eliminate materials outside of the budget and green checks were assigned for those materials that were feasible.

- **Ease of Synthesis and Processability:** The materials that were easy to synthesize or easy to incorporate in the design received a green check whereas the materials that needed prior modification before they could be used received a red x.
- **Insulating/Conductivity:** Depending on the function of the material class, the ability to either conduct or insulate electrons was evaluated. If the material effectively performed its function it received a green check mark.
- **Enzyme Immobilization:** The ability of the material to be immobilized with the enzyme used for the reactions was evaluated. If the material showed poor immobilization of the enzyme it received a red x.
- **Stability:** The system needs to be stable for 21 days, therefore the material received a green check if there was literature supporting that its stability *in vivo* is at least 21 days.

## Appendix 4.C: Monitoring Ability Evaluation

Monitoring Ability (40 points total)												
DESIGN	1	2	3	4	5	6	7	8	9	10	11	12
Precision	6	6	6	3	6	6	3	3	6	6	6	3
Sensitivity	9	13	9	11	9	9	9	13	3	6	6	9
Selectivity	13	13	13	13	13	13	13	13	13	13	13	13
Response Time	2	2	2	2	2	2	2	2	2	1	1	1
Stability	2	6	6	4	2	4	4	3	6	2	2	4
Total:	32	40	36	33	32	34	31	34	30	28	28	30

The team decided to assign scores in each category based on relative expected performance to each other. This ranking system resulted in the following breakdown:

- **Precision:** Designs receiving a 3 ran the risk of creating a local environment inside the biosensor system that would not accurately reflect the GBM tissue metabolite concentrations due to a membrane covering an inner layer. The designs receiving a 6 did not encounter this problem
- **Sensitivity:** Scores for sensitivity were assigned as follows:
  - 13 if coating considered superconductive
  - 11 if coating consisted of both a gel and a membrane, as the two structures would serve to trap any hydrogen peroxide attempting to exit the sensing area.
  - 9 if only a membrane was present in the design.
  - 6 if the design was porous, as the porous structure would better trap hydrogen peroxide.
  - 3 if the design contained no construct that could contain exiting hydrogen peroxide
- **Selectivity:** Each of the designs received a 13 for selectivity, as they all utilized enzymes as the bioselective agent.
- **Response Time:** Designs that took advantage of the secondary enzyme HRP scored a 2 in this category while designs that did not received a 1. This is because the HRP

will speed up the breakdown of hydrogen peroxide into free electrons that can be directly measured.

- **Stability:** The stability was ranked by how each design was perceived to trap the H<sup>+</sup> ions generated by the hydrogen peroxide breakdown. A decrease in pH due to the production of these ions would break down the coating faster, making it less stable. Scores were assigned as follows:

- 6 if no membrane or pores in design.
- 4 if the design contained a membrane.
- 2 if the design was porous
- 1 If the design had both a porous structure as well as a membrane.



## Appendix 4.D: Manufacturability Evaluation

Manufacturability (30 points total)												
DESIGN	1	2	3	4	5	6	7	8	9	10	11	12
Reproducibility	4	5	5	2	4	3	2	3	3	4	4	3
Ease of Production	20	5	8	15	25	15	10	18	5	20	25	15
Total:	24	10	13	17	29	18	12	21	8	24	29	18

The manufacturability scores were assigned in a similar way as the monitoring scores, and resulted in the following breakdown:

- **Reproducibility:** The reproducibility was assigned based on the ability of the design to be identically manufactured and scores were given based on the following criteria:
  - 5 if each manufactured coating could be precisely controlled.
  - 4 if the the coating contained one layer, since each iteration could be created similarly.
  - 3 if the coating contained a membrane.
  - 2 if the design consisted of either 3 layers or was a smart polymer. These designs would vary the greatest between biosensors.
- **Ease of Production:** The ease of production score was assigned based on the team's ability to synthesize the coating. Scores were given as follows:
  - 25 if the design only consists of a single layer
  - 20 for a design that contains the mushroom
  - 15 for a bilayer and polycarbonate membrane
  - 10 for a trilayer design
  - 8 for a design with CNTs and only single layer
  - 5 for a design with aligned CNTs or nanohooks

## Appendix 4.E: Interference Evaluation

Interference (20 points total)												
DESIGN	1	2	3	4	5	6	7	8	9	10	11	12
Isolating from environment	5	0	5	10	0	10	10	0	10	5	0	10
Isolating reaction products	5	10	0	5	0	5	10	0	10	5	0	5
Total:	10	10	5	15	0	15	20	0	20	10	0	15

The designs for this category were scored as follows:

- Isolating from environment:** This category ranked how well the design functioned to keep potentially interfering agents (i.e. electroactive particles or free hydrogen peroxide) out of the sensing area of the biosensor. Designs that included a membrane were deemed to work best and received a score of 10. The two mushroom designs as well as the CNT bed designs received a 5 since their non-conductive coatings shield the electrode. Designs that provided no way to isolate from interfering agents received a 0.
- Isolating breakdown products:** This category was based on how well the device could trap the hydrogen peroxide and free electrons generated from the enzymatic reactions. A 10 was assigned to the Trilayer, CNT towers, and Nanovelcro designs since these designs performed this function best. A 5 was given to designs that only contained a membrane or to the mushroom design and a 0 to designs that did not contain any mechanism to trap the reaction products.

#### Appendix 4.F: Cost Evaluation

The total cost for each of the designs was determined by adding together the costs of each of the individual materials used to create it. The conductive material price is for polypyrrole and the non-conductive price for chitosan. For numbers that are bolded, this indicates that the material used deviated from the normal material used in all design alternatives. Bolded conductive numbers are for a smart polymer and bolded non-conductive for a polycarbonate membrane. A1 indicates that the design utilizes the material class and a 0 indicates that it does not.

Design	Conductive	Price/g	Non-Conductive	Price/g	CNT	Price	HRP	Price	Total
<b>Musroom</b>	1	\$21.06	1	\$ 2.86	0	\$300.00	1	\$74.4	\$ 98.32
<b>CNT Towers</b>	1	\$ 21.06	0	\$2.86	1	\$300.00	1	\$74.4	\$ 395.46
<b>CNT Bed</b>	0	\$21.06	1	\$2.86	1	\$300.00	1	\$74.4	\$ 377.26
<b>Smart Polymer</b>	<b>1</b>	<b>\$ 12.82</b>	<b>1</b>	<b>\$ 70.00</b>	0	\$300.00	1	\$74.4	\$ 157.22
<b>Single Layer</b>	1	\$21.06	0	\$ 2.86	0	\$300.00	1	\$74.4	\$ 95.46
<b>Bilayer</b>	1	\$21.06	1	\$ 2.86	0	\$300.00	1	\$74.4	\$ 98.32
<b>Trilayer</b>	1	\$21.06	1	\$2.86	0	\$300.00	1	\$74.4	\$ 98.32
<b>Single Layer Indent</b>	1	\$21.06	0	\$2.86	0	\$300.00	1	\$74.4	\$ 95.46
<b>Nanovelcro</b>	1	\$21.06	<b>1</b>	<b>\$ 70.00</b>	0	\$300.00	1	\$74.4	\$ 165.46
<b>1 Enzyme Mushroom</b>	1	\$21.06	1	\$ 2.86	0	\$300.00	0	\$74.4	\$ 23.92
<b>1 Enzyme Single Layer</b>	1	\$21.06	0	\$ 2.86	0	\$300.00	0	\$74.4	\$ 21.06
<b>1 Enzyme Bilayer</b>	1	\$21.06	1	\$ 2.86	0	\$300.00	0	\$74.4	\$ 23.92

The score breakdown was as follows:

- 10 was assigned to the lowest costing material out of all design alternatives.
- 9 was given if the total cost was under \$50.
- 7.5 was given if the total cost was between \$50-\$100
- 5 was given if the total cost was between \$100-\$200
- 2.5 was given if the total cost of the design exceeded \$200

Cost (10 points total)												
DESIGN	1	2	3	4	5	6	7	8	9	10	11	12
Cost	7.5	2.5	2.5	5	7.5	7.5	7.5	7.5	5	9	10	9
Total:	7.5	2.5	2.5	5	7.5	7.5	7.5	7.5	5	9	10	9

## Appendix 5.A: Protocol for Polypyrrole Deposition

### Preparing Pyrrole/ KCL stock solution

1. Measure 0.034g of Pyrrole powder into a 20ml glass vial tube and add 10ml of 0.1M KCL.
2. Degass the solution using Nitrogen for 30 minutes at 80psi. Make sure the pipette tip is placed in the liquid.

### Electrodeposition of the Polypyrrole film

1. Immerse the working and reference electrode into the Pyrrole/ KCL stock solution.
2. Make sure the electrodes do not touch the bottom or the sides of the glass vial.
3. Attach the red alligator clips to the working electrode and the blue alligator clips to the reference electrode (as shown in Figure 32).



Figure 33: Setting up the biosensor for PPy deposition

### Operating the GPES software

1. Before running the software, make sure that the Autolab PGSTA12 is powered on and re-calibrated
2. Open the GPES software and use the amperic method.
3. Run the current for 30minutes (1800secs) at 0.75 Hz.
4. Data or graph generated measures current against time.
5. After 30minutes, remove the working electrode and gently wash the electrode using DI water.

6. Compare the Polypyrrole coated working electrode to a clean uncoated working electrode.

### **Cleaning the electrode**

#### **\*\*Should be cleaned before each deposition**

- 1) Place a small amount of 0.1 micron and 1micron aluminum slurry onto separate circular scouring pads.
- 2) Add small drops of DI water to the pads.
- 3) On each pad, move the electrode counter-clockwise for 3 minutes.
- 4) Wash the electrode with DI water and ethanol to remove the powder residue.
- 5) Place the electrodes into a beaker of DI water and sonicate for 5 minutes.
- 6) Place the electrodes into a beaker of ethanol and sonicate for 5 minutes.
- 7) Allow the electrode to air-dry.

### **Protocol for Enzyme Immobilization**

- 1) 2.5mg of the lactate oxidase powder was added to 1mL of DI water.
- 2) The enzyme is then aliquot into 0.5mL centrifuge tubes, then stored into a -20°C fridge.
- 3) Add 30µl of the enzyme into the degassed pyrrole/KCL and vortex.
- 4) Repeat the steps for the protocol for Electrodeposition.

## Appendix 5.B: Contact Angle Analysis

- 1) Turn on the Rame-Hart Auto Dispensing system and the Schott to 70.
- 2) Take the lens cover off of the camera.
- 3) Open the DROP Image Standard software.
- 4) Press 'yes' for Reset.
- 5) Press the square for live image.
- 6) Ensure the DI water bottle is sufficiently filled.
- 7) Click on Drop Volume Control.
- 8) Choose Drop option and Rinse at least once and press the start button.
- 9) Change to reservoir option and press fill on the right.
- 10) Put the syringe on the metal platform.
- 11) Attach sample to side of platform using tape.
- 12) Ensure sample is in line of view of camera and that surface is perpendicular to camera.
- 13) Change the volume step in the software to 2 microliters.
- 14) Place one drop of water onto sample surface
- 15) Click the Contact Angle tool in software.
- 16) Click start and click on picture.
- 17) Place COLOR line to the left of drop applicator by left clicking.
- 18) Place COLOR line to the right of drop applicator by right clicking.
- 19) Place COLOR line flush with surface of sample using the up and down arrows of the keyboard.
- 20) Click measure. Left, right, and mean contact angle values will be calculated.
- 21) Close software and machines. Place the lens cover onto camera.

## Appendix 5.C: Cyclic Voltammetry

- 1) Start the GPES software.
- 2) Click on the procedure tab, located on the top left hand section on the panel.
- 3) Click Cyclic Voltammetry and then click Normal
- 4) Enter following parameters into interactive screen:
  - a. Starting Voltage: -0.2 V
  - b. Initial voltage: -0.2V
  - c. Final Voltage: 0.6V
  - d. Speed: 1 V/s
  - e. Select current between 10nA to 100mA
- 5) Click start and then continue buttons located at the bottom right hand corner of the screen.



## Appendix 5.D: Lactate Amperometry

### Preparation

- 1) Deposit a PPy film with 30 $\mu$ L enzyme (refer to film deposition protocol 5.A for details).
- 2) Establish which concentrations of lactic acid solution are being tested.
- 3) Label 50 mL conical tubes with desired lactic acid concentrations.
- 4) Dilute the lactic acid to the desired concentrations using DI water.
- 5) Add 10mL of desired concentration of lactic acid into a 20mL beaker.
- 6) Place stir bar in beaker and beaker onto stir plate at setting 4.
- 7) Place the working electrode (WE) in the beaker, followed by the reference electrode (RE) and the counter electrode (CE).

### Testing

- 8) Set up the amperometry GPES program at a voltage of -.2 for 120 seconds
- 9) Press start.
- 10) After the 120 seconds, double click just above the lines on the graph and a table with the data points will appear. Copy the data points into an excel file made for this particular experiment.
- 11) Repeat 3 times to prove reproducibility of results.

\*Use a fresh electrode with PPy film and enzyme for each test

## Appendix 5.E: Real Time Lactate Recognition

### Preparation

- 1) Deposit a PPy film with 30 $\mu$ L enzyme (refer to film deposition protocol for details).
- 2) Prepare XX mL of **XX $\mu$ X** of lactic acid.
- 3) Obtain a 20mL beaker with 10mL of DI water
- 4) Place beaker with stir bar on stir plate on setting 4
- 5) Place the working electrode (WE) in the beaker, followed by the reference electrode (RE) and the counter electrode (CE).

### Testing

- 6) Set up the amperometry GPES program at a voltage of -.2 for 120 seconds
- 7) Press start and wait 60 seconds, then administer the first 1mL drop of lactic acid.
- 8) Drop 1mL of lactic acid every 20 seconds for 120 seconds.
- 9) After the 120 seconds, double click just above the lines on the graph and a table with the data points will appear. Copy the data points into an excel file made for this particular experiment.
- 10) Repeat 3 times to prove reproducibility of results.

\*Use a fresh electrode with PPy film and enzyme for each test

## Appendix 5.F: Colorimetric Lactate Assay

### Standards

- 1) Dilute 10 mL of the 100 nmole/mL Lactate standard with 990 mL of Lactate Assay Buffer to generate a 1 nmole/mL standard solution.
- 2) Add 0, 2, 4, 6, 8, and 10 ml of the 1 nmole/mL Lactate standard into a 96 well plate, generating 0 (blank), 2, 4, 6, 8, and 10 nmole/well standards.
- 3) Add Lactate Assay Buffer to each well to bring the volume to 50 mL.

### Media Samples

- 1) Deproteinized media samples with a 7kDa MWCO spin filter to remove lactate dehydrogenase.
- 2) Add 50uL of media to the wells of the 96 well plate.
- 3) Add 50uL of the Master Mix to each well to bring the total volume to 100uL. The Master Mix contains: Lactate Assay Buffer (46 mL), Lactate Enzyme Mix (2 mL) and Lactate Probe (2 mL).
- 4) Mix well and incubate at room temperature for 30 minutes, protected from light.
- 5) Read the absorbance value at a wavelength of 570nm.

### **Appendix 5.G: Biosensor in Media**

- 1) Using media collected from cell culture and freshly deposited electrodes with PPy run the Amperometry GPES software.
- 2) Place electrode in 4mL of desired media and run test for 2 min at  $-0.2V$